Nanostructures

DOI: 10.1002/anie.201402890

Formation of Nanoparticles and Nanostructures—An Industrial Perspective on $CaCO_3$, Cement, and Polymers

Jens Rieger, Matthias Kellermeier, and Luc Nicoleau*

Keywords:
cement · materials science · nanoparticles · nanotechnology · silicates

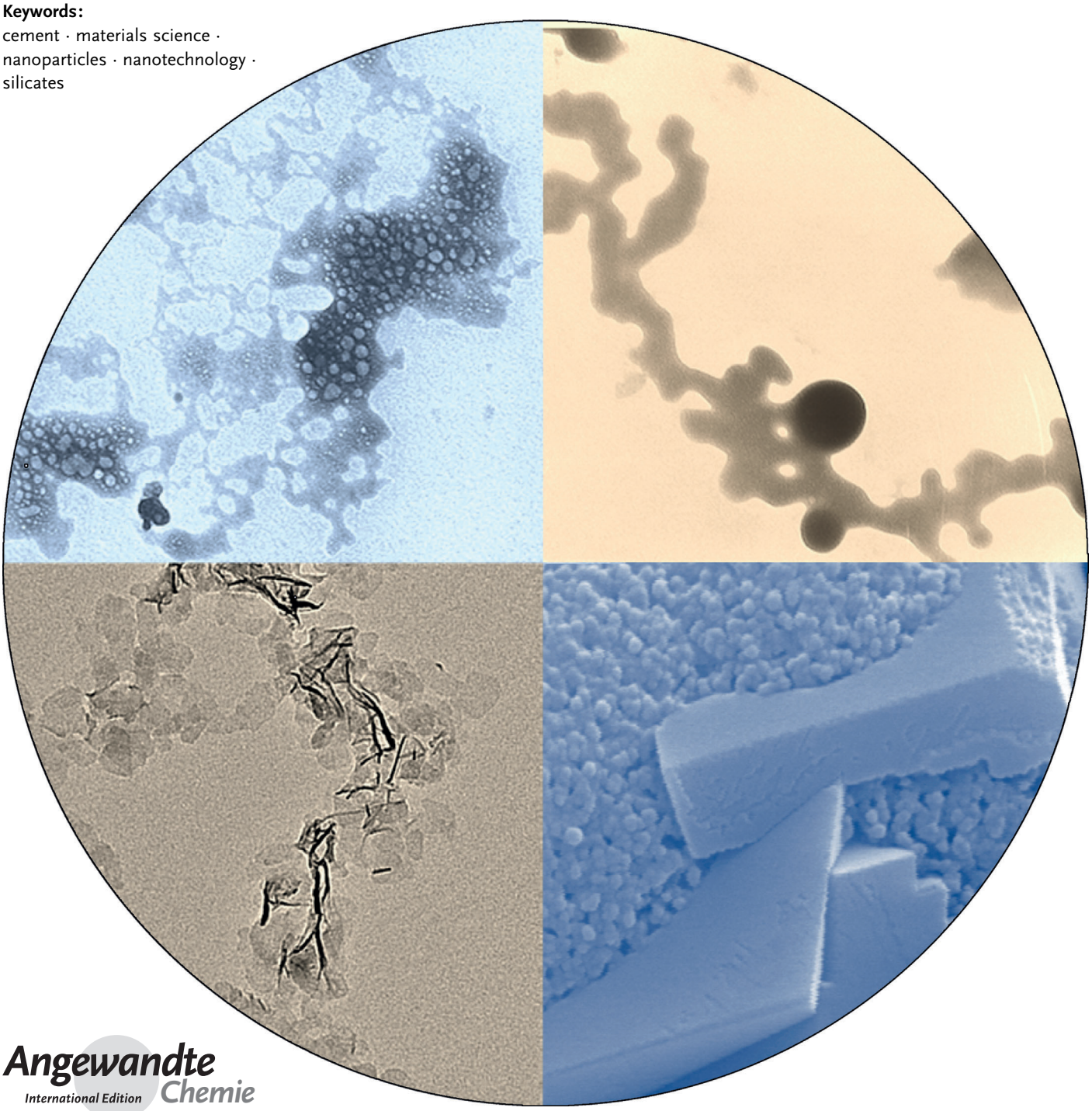

Nanotechnology enables the design of materials with outstanding performance. A key element of nanotechnology is the ability to manipulate and control matter on the nanoscale to achieve a certain desired set of specific properties. Here, we discuss recent insight into the formation mechanisms of inorganic nanoparticles during precipitation reactions. We focus on calcium carbonate, and describe the various transient stages potentially occurring on the way from the dissolved constituent ions to finally stable macrocrystals—including solute ion clusters, dense liquid phases, amorphous intermediates, and nanoparticles. The role of polymers in nucleating, templating, stabilizing, and/or preventing these structures is outlined. As a specific example for applied nanotechnology, the properties of cement are shown to be determined by the formation and interlocking of calcium-silicate-hydrate nanoplatelets. The aggregation of these platelets into mesoscale architectures can be controlled with polymers.

From the Contents

1. Introduction

Nanotechnology provides a unique approach to create specific properties of a material by preparing it in the form of nanoparticles or with a suitable nanostructure. Examples of such properties are color, reactivity, magnetism, and bioavailability, which differ in many cases from the behavior of both the corresponding bulk material and the constituting molecules. These specific nanoeffects have been used for the development of a large number of products in the fields of advanced materials and coatings, catalysis, electronics, energy and water management, sensors, drug delivery, and other medical applications.[1] A much less frequently discussed aspect of nanotechnology—which represents the actual topic of this Review—is its importance in materials and soft matter science, where the formation of nanostructures is an integral part of solidification and formulation processes. In this context, we have chosen two model systems: the crystallization of an extensively studied inorganic mineral, calcium carbonate, and—even more specific—the hydration of cement-silicate phases. Knowledge gained from these prominent examples should also be applicable in other areas, where self-organizing or bottom-up principles are employed to determine the properties of a material by tailoring its nanostructure. Nature provides the most intriguing archetypes for successful, and seemingly perfect, control over solidification at the nanoscale, yielding hierarchical hybrid structures with outstanding and task-specific performance, as found, for example, in bone and teeth.[2]

It should be stressed that the term nanotechnology not only covers the synthesis/fabrication of nanoparticles but also, and more generally, the preparation of bulk materials and films with specific nanostructures. This aspect is taken into account by the following definitions:[3] "Nanotechnology: Application of scientific knowledge to manipulate and control matter in the nanoscale, where size- and structure-dependent properties and phenomena, as distinct from those associated with individual atoms or molecules or with bulk materials, can emerge," and "Nanoscale: size range from approximately 1 nm to 100 nm." Apart from the broader definition of nanotechnology covering one-, two-, and three-dimensional systems, and not only nanoparticles, it is important to realize that one of its key elements is the understanding of how to design matter on the nanoscale with the desired specific properties; that is, (nano-)structure–property relationships represent a focal point of nanotechnology.

In this Review, we address the above points from two distinct perspectives: 1) it is shown how the picture of nanoparticle formation in precipitation reactions has changed over the past years through the observation of transient nanostructures and how we may benefit from these findings to create new materials. 2) In hydrated cement, which is a true multiscale material, nanostructures play a key role in both the setting and the hardening phases; here we describe the current state of knowledge and outline approaches to control structure formation at the nanoscale.

2. Formation of Nanoparticles and Nanostructured Materials

Crystallization in itself is a crucial step in the production and processing of many materials, such as catalysts, pharmaceuticals, pigments, and concrete,[4,5] as well as for the occurrence of minerals in natural environments, both in their inanimate form[6] and associated with living organisms.[7] This is one of the reasons why crystallization has been intensively investigated for decades.[8] However, it is generally accepted that many properties of an emerging solid phase can essentially already be determined at the onset of precipita-

[*] Dr. J. Rieger
Advanced Materials and Systems Research, BASF SE
GM/I—B1, 67056 Ludwigshafen (Germany)
E-mail: jens.rieger@basf.com
Dr. M. Kellermeier
Material Physics, BASF SE
GMC/O—G201, 67056 Ludwigshafen (Germany)
Dr. L. Nicoleau
Construction Materials and Systems
BASF Construction Solutions GmbH
GMB/M—B08, 83308 Trostberg (Germany)

tion, that is, at the nanoscale. Moreover, there is increasing evidence that in most cases, crystallization does not proceed through a simple one-step pathway directly from the dissolved monomeric constituents to the macroscopically stable crystalline phase, but rather involves a series of precursor and intermediate species that successively transform into one another.[9–12] Clearly, such multistep reaction pathways implicate additional and previously not recognized possibilities to steer the progress of crystallization in certain desired directions. Figure 1 provides an overview of the various stages that have recently been discussed to occur during the formation of (nano)particles from supersaturated solutions, and which will be addressed in more detail below.

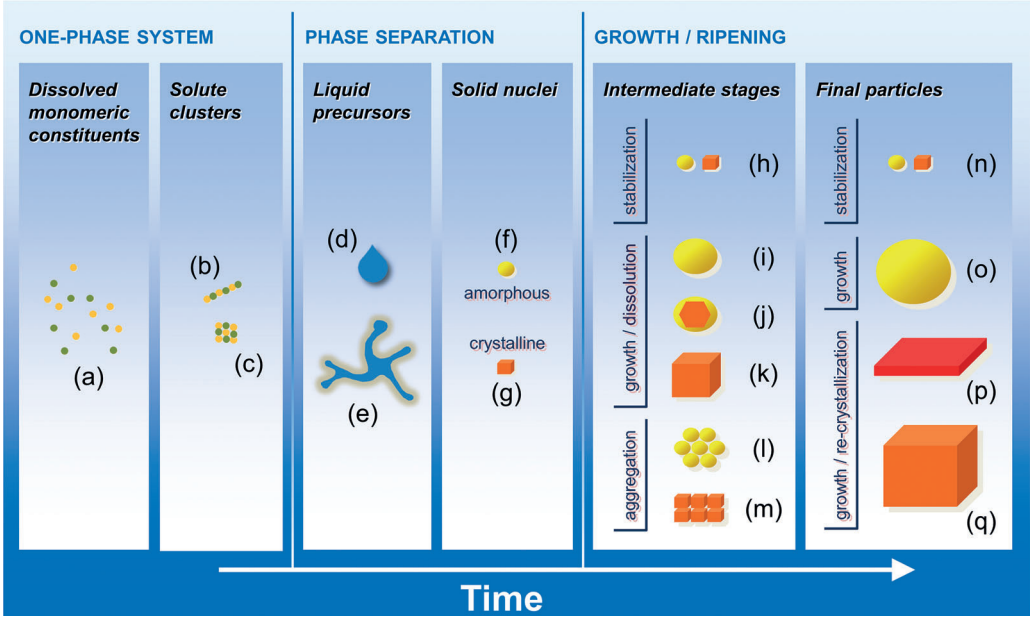

Figure 1. The various stages that have been proposed to occur during nanoparticle formation and crystallization of both inorganic and organic compounds from solution. In the homogeneous one-phase system, dissolved monomeric units (e.g. cations and anions; a) may undergo association into solute clusters with chainlike (b) or more compact structures (c). Once a critical level of supersaturation is reached, phase separation will take place, resulting in dense liquid droplets (binodal (l)-(l) demixing; d), bicontinuous liquid patterns (spinodal (l)-(l) decomposition; e), or solid nuclei (binodal (s)-(l) demixing) with either amorphous (f) or crystalline (g) structure. Over time, the liquid precursors and/or solid nuclei evolve into nanoparticles that can be stable (h), grow into larger amorphous (i) or crystalline (k) particles, potentially involving amorphous-to-crystalline solid-state transformations (j), or aggregate in a random (l) or ordered (m) fashion. Further ripening ultimately affords the final product, which can be a stable colloidal suspension of nanoparticles (n), micrometer-sized amorphous particles (o), or crystals with various habits (p,q), depending on the boundary conditions and the presence of additives.

The most fundamental and important step in the evolution of any solid particle is the actual process of phase separation, that is, nucleation. Interestingly, despite continuous research in this area, it is still quite common to analyze data taken from precipitation experiments by means of classical nucleation theory (CNT), which in its original form was developed almost 100 years ago[13] and has since been the subject of numerous books and reviews.[6,14] The popularity of this approach is due, on the one hand, to the conceptual simplicity of CNT. On the other hand, deeper insight into the nucleation process is usually limited because of the difficulty to experimentally access the very early stages of crystallization with the necessary temporal and spatial resolution of, at least, milliseconds and nanometers, respectively. However, only with a profound understanding of these first steps—which often differ from the picture suggested by classical theories of nucleation and growth—will full control over crystallization become possible. In fact, CNT frequently fails to correctly predict quantitative values for real systems.[15] One explanation for these shortcomings lies in the sequential precipitation scenario depicted by Figure 1, that is, the initially nucleated phase may be substantially different from the finally obtained solid one (as shown more explicitly for

Jens Rieger received his PhD in 1989 in Theoretical Physics and joined BASF, where he has been involved in R&D projects in the fields of plastics, coatings and paints, foams, cosmetics, pharma formulations, etc. As Senior Vice President he is responsible for scouting and implementing new technologies in the field of Advanced Materials & Systems Research. He is Distinguished Guest Professor at the Changchun Institute of Applied Chemistry (Chinese Academy of Sciences) and Visiting Scientist at Harvard University.

Matthias Kellermeier obtained a PhD in Physical Chemistry from the University of Regensburg in 2011, for which he was awarded the Starck Prize for Solid-State Chemistry and Materials Research. After postdoctoral research with Prof. Helmut Cölfen at the University of Konstanz, he joined BASF in 2013 as a Research Scientist in the Materials Physics Department. His research interests range from biomimetic crystallization and self-assembly over general mechanisms of nucleation to the physical characterization of surfaces.

calcium carbonate below). Another reason is that the properties of a given phase can change when the particle size is decreased to nanoscopic dimensions. For example, the tendency of macroscopically metastable phases to exhibit lower surface energies than their stable counterparts could lead to a crossover in thermodynamic stability at the nanoscale (where the surface-to-bulk ratio is high).[16–18] While this may rationalize the empirical step rule of Ostwald,[19] there is still one central problem, namely that the nature of size-dependent variations in phase energetics is currently not known.[20] For further discussions on extensions and limitations of CNT, the interested reader is referred to the articles by Erdemir et al.[21] and Sear.[22]

2.1. Prenucleation Clusters

A fundamental consequence of classical nucleation theory is that nuclei, or clusters, should not exist to any significant extent in solution prior to particle formation. Evidence arguing against this notion was already reported decades ago for certain organic compounds.[23] In the case of calcium carbonate, it has long been conjectured that ion pairing leads to an equilibrium population of associated species in solution next to the free ions (stages (a)–(c) in Figure 1).[24] In more recent work, it was demonstrated that association proceeds beyond simple ion pairs and instead affords a distribution of larger clusters comprising as many as several tens of $CaCO_3$ units.[25–27] The presence and size of these species was inferred from analytical ultracentrifugation[25] and high-resolution cryo-TEM experiments.[28] In addition, by tracking calcium activities in titration-based precipitation assays, it could be shown that such ion clusters are not at all rare in solution, but in fact represent a preferred state in thermodynamic equilibrium.[25] In other words, these so-called "prenucleation clusters" appear to be stable solute complexes that exist within the boundary of a one-phase system, rather than solid particles or nuclei—all completely at odds with the concepts of CNT.[27] Computer simulations have confirmed the thermodynamic stability of prenucleation clusters and moreover indicate that they are ionic polymers, composed of chains of alternating calcium and carbonate ions, which may adopt linear, ringlike or branched structures (see stage (b) in Figure 1).[29]

Luc Nicoleau completed his PhD at the University of Dijon in the group led by Prof. A. Nonat. In 2005, he started postdoctoral research at the LCPP in Lyon. He joined BASF in 2006 and since 2009 he has been a Senior Scientist in the construction chemicals research group. He specialized in the hydration of hydraulic binders and the interactions between polymers and cementitious materials. His research is focused on the development of stabilized cement hydrates for use as hardening accelerators, and the control over the mechanical properties of concrete and geopolymer materials.

Although ion association in $CaCO_3$ solutions seems now to be broadly accepted in the community, the sheer existence of any such clusters does not have a direct bearing on nucleation, that is, these species do not necessarily act as precursors of crystals.[26] However, there is evidence suggesting that under certain conditions they may become relevant for nucleation, namely by aggregation in solution,[25,28] to give diffuse entities (ca. 30 nm) that later appear to transform into solid nanoparticles of amorphous calcium carbonate (ACC)[30] (i.e. a pathway along steps (a), (b), and (f) in Figure 1).

The discovery of prenucleation clusters has spurred a great deal of research related to early stages of crystallization over the past few years, also on compounds other than $CaCO_3$, such as calcium phosphate[31] and amino acids.[32] However, the concept of these clusters and their actual role in phase separation is still heavily debated; a comprehensive recent update on this topic is provided by Gebauer et al.[27] and Kellermeier et al.[33]

2.2. Liquid–Liquid Phase Separation

Another fact that opposes the classical picture of nucleation is the observation of liquid precursors during crystallization, presumably formed by demixing of a supersaturated and originally homogeneous solution into two liquid phases, one rich and one poor in solute. In the case of calcium carbonate, it was Faatz et al.[34] who first speculated that spherical nanoparticles of ACC—which represent the initial phase observed upon $CaCO_3$ nucleation under most experimental conditions[11,35]—could form through a liquid–liquid demixing process. They proposed a hypothetical phase diagram with a lower critical solution temperature (LCST; Figure 2), which comprises stable homogeneous regions at both low (A) and high (F) solute concentrations, metastable binodal regimes (B-C and D-E) where phase separation is thermodynamically favored, as well as a spinodal area in which the system becomes unstable and will decompose spontaneously.

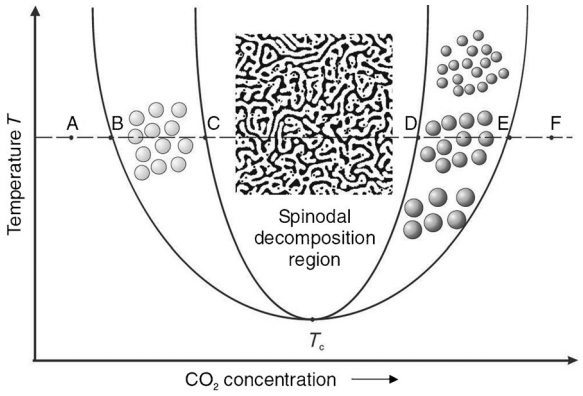

Figure 2. Schematic phase diagram of the aqueous calcium carbonate system suggested by Faatz et al. (the horizontal axis represents the composition). For further explanations see the text (reproduced from Ref. [34] with permission from John Wiley & Sons, Copyright 2004).

Conceptually, liquid–liquid phase separation in the binodal regime is equivalent to nucleation in the classical sense, with the sole exception that a liquid instead of a solid phase is nucleated. Binodal demixing is expected to yield (spherical) droplets of the new liquid phase dispersed in the mother solution (stage (d) in Figure 1), which may subsequently transform into solid particles by progressive dehydration. This pathway has been discussed by Wolf et al. to explain the liquidlike appearance of carbonate nanoparticles isolated from contact-free crystallization experiments in an acoustic levitator.[36] However, these observations were made after drying the specimens on a solid support, which may potentially lead to structural changes. Later, Bewernitz et al. were able to actually prove the liquid character of early $CaCO_3$ precursors in situ by means of NMR spectroscopy.[37] Interestingly, precipitation was carried out in all of these studies by gradually increasing the supersaturation at a rather low pH value. One may thus speculate that dense liquid phases indeed occur generally as transient intermediates in $CaCO_3$ crystallization, but their particular lifetime—and hence experimental detectability—depends on specific conditions, such as the presence of intrinsically stabilizing bicarbonate ions.

Similar mechanisms were also proposed for other mineral systems, as for example in the case of magnesium sulfate, where $MgSO_4$ polymers appeared to form in phase-separated solute-rich droplets under hydrothermal conditions.[38] Dense liquid clusters are, moreover, common in the field of protein crystallization, where mesoscopic entities enriched in protein play a key role in the so-called two-step mechanism of nucleation.[39]

Spinodal decomposition, on the other hand, is presumed to produce more complex bicontinuous patterns (see inset in Figure 2 and stage (e) in Figure 1). In the case of calcium carbonate, potential signatures of this inherently unstable state could be traced by ultrafast quenching of the very early stages of precipitation, as shown in Figure 3:[11] initially, a disordered emulsion-like structure forms (Figure 3a), which then becomes coarser over time to yield nanosized amorphous spheres (Figure 3b). The existence of emulsion-like intermediate states as a possible result of spinodal phase separation or, alternatively, structure formation upon (turbulent) mixing of the reactant solutions, is still a matter of debate; to our knowledge, the sole direct experimental support for a spinodal mechanism is based on cryo-TEM data, which should be interpreted carefully because of possible structural rearrangements during vitrification of the sample. Early attempts to use small-angle X-ray scattering to track the development of the precipitating systems in situ unfortunately did not provide unequivocal evidence for this phenomenon.[40] However, cryo-TEM studies performed in an independent, more recent study again provided hints for liquid–liquid demixing in supersaturated calcium carbonate solutions, as smooth networks of electron-dense regions (presumably a $CaCO_3$-rich phase) with liquidlike morphologies were found interspersed in a less-dense matrix (residual $CaCO_3$-depleted bulk solution).[41] In addition, similar morphological evolution—from phase-separated emulsion-like states to coarsened particle shapes—was also traced during the precipitation of quinacridone, an organic pigment, and boehmite (aluminum oxohydroxide).[40] Thus, there are several experimental observations that argue for the relevance of spinodal demixing pathways in mineralization, but clearly, more work needs to be done to fully elucidate the detailed underlying mechanisms.

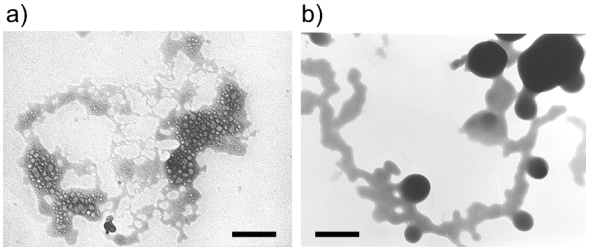

Figure 3. Cryo-TEM micrographs of calcium carbonate precipitation about a) 100 ms and b) 2 min after mixing 0.01 M solutions of $CaCl_2$ and Na_2CO_3. Scale bars: 200 nm (reproduced from Ref. [11] with permission from the Royal Society of Chemistry, Copyright 2007).

Substantial support for liquid–liquid phase separation being a viable pathway for $CaCO_3$ nucleation comes from recent computer simulations.[42] Wallace et al. were able to model the growth of small clusters into larger entities that exceed the presumed critical size. It was found that the initially dynamic solute species rapidly evolve into more condensed states as further ions are added. The calculated ion diffusivities decreased with growing cluster size, but remained markedly higher than in solid ACC. This suggests that the clusters become less dynamic as the driving force for phase separation increases, and at some point transform into droplets of a dense ion-rich liquid phase. Subsequent agglomeration and dehydration/solidification would then produce amorphous nanoparticles, in line with what is observed experimentally.[43] Another important result of the simulations by Wallace et al. is that the free energy decreases continuously with increasing cluster size, and that there is no significant barrier to both the growth and association of the clusters.[42] This was taken as an indicator for spinodal decomposition into a dense liquid phase and the formation of an ion-depleted bulk solution being the actual mechanism of nucleation under the conditions of the simulations (i.e. at 0.015 M $CaCO_3$)—which, interestingly, were close to those chosen in the study represented in Figure 3.[11] From an experimental point of view, it is intuitive to assume that the spinodal region can only be reached if a high level of supersaturation is established in a sufficiently short frame of time (i.e. by rapid mixing of solutions at high concentration and/or pH value), so that the system can pass the binodal regime and becomes unstable against density fluctuations, thereby leading to emulsion-like structures, as described in Figure 3. In practice, it is well known that nucleation often requires an energetic barrier to be overcome, especially at lower supersaturation. Thus, while spinodal decomposition may occur under certain conditions, it can hardly serve as a general mechanism for calcium carbonate nucleation. Further details and controversial discussions on this fascinating topic can be found elsewhere.[27]

2.3. Amorphous Nanoparticles and Their Transformation to Crystalline Polymorphs

Regardless of the particular pathways leading to nucleation, the precipitation of calcium carbonate from aqueous solutions frequently affords amorphous nanoparticles as the first solid product, as already mentioned in the previous section. This has been confirmed for various experimental conditions, including fast reactions at high supersaturation[11,44,45] (Figure 4a) and elevated pH values,[46] as well as

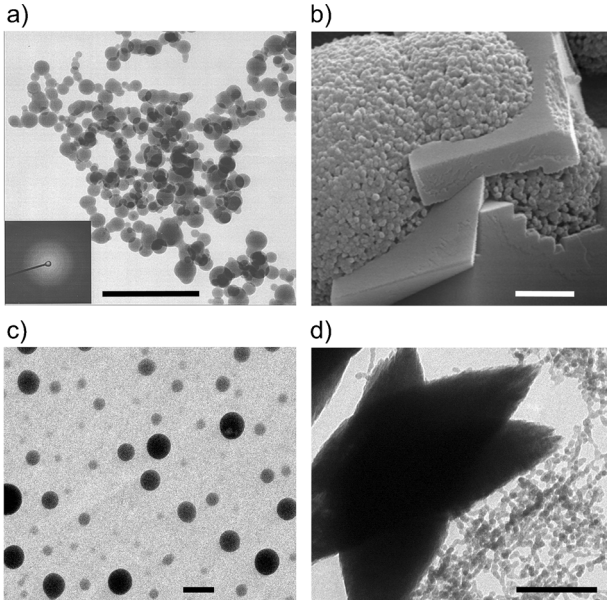

Figure 4. a) Cryo-TEM and b) SEM images showing the progress of calcium carbonate precipitation about a) 1 min and b) 10 min after mixing 0.01 M solutions of $CaCl_2$ and Na_2CO_3. Scale bars: 1 μm. Reproduction of (a) from Ref. [11] with permission from the Royal Society of Chemistry, Copyright 2007, and (b) from Ref. [64], Copyright 2002 Carl Hanser Verlag, München. c,d) Cryo-TEM micrographs of zinc oxide/hydroxide particles observed c) 6 min and d) 15 min after precipitation was initiated. Scale bars: 200 nm (unpublished data).

slow mineralization under diffusion- or reaction-controlled processes.[34,47] Moreover, there are various approaches to enhance the yield and/or lifetime of ACC in solution syntheses, for example, by adding magnesium ions,[48] by quenching in ethanol,[49,50] through confinement of the reaction space,[51] or by introducing certain additives, most notably polymers[52] (which will be discussed in more detail in the following section), but also small molecules,[53] surfactants,[54] proteins,[55,56] and inorganic silicate.[44] An interesting observation in this context is that there appears to be more than one structural form of amorphous calcium carbonate, a phenomenon that has been known for biogenic samples of ACC for quite some time.[57] On the one hand, the amorphous phase can have distinct degrees of hydration, which affect its (meta)stability and may also be important for the transformation into more stable states.[58,59] On the other hand, it was shown that the short-range structural order of solid ACC materials can vary depending on the conditions chosen for their preparation, a behavior recently denoted as polyamorphism.[60] For example, ACC particles obtained from solutions at modest levels of supersaturation were found to exhibit structural features that to some extent resembled the regular order observed in the crystalline polymorphs calcite and vaterite.[49] Furthermore, pressure treatment led to the formation of an ACC phase with a protostructure reminiscent of aragonite.[61] In turn, a different structural model—suggesting a calcium-rich framework with channels containing water and carbonate ions—was proposed for ACC precipitated from solutions at higher supersaturation.[62]

If no specific measures are taken to stabilize the ACC particles, the material will ultimately transform into the thermodynamically stable form (stages (i)–(k) and (o)–(q) in Figure 1), which is calcite under ambient conditions. This process may involve vaterite as an intermediate phase,[11,63] which typically occurs as roughened aggregates of small nanoparticles and eventually gives way to smooth rhombohedral crystals of calcite (Figure 4b).[11,45,64] However, calcite can also be formed directly from ACC without vaterite as an intermediate.[44] To illustrate that amorphous precursors and metastable crystalline intermediates are not unique to $CaCO_3$ crystallization, we present here also the case of zinc oxide, which was precipitated by mixing 0.05 M solutions of zinc nitrate and sodium hydroxide at 40 °C: initially, spherical amorphous nanoparticles are formed (Figure 4c), which first transform into a granular structure with a feature size of about 20 nm (presumably zinc hydroxide), and then to the thermodynamically stable crystalline form, that is, hexagonal wurtzite-type ZnO (Figure 4d). Another system exhibiting fairly complex precipitation behavior is calcium sulfate, an abundant natural mineral that is used on large scales for construction applications. Here, very recent studies have suggested that the stable modification (gypsum, $CaSO_4{\cdot}2H_2O$) does not crystallize directly from aqueous solutions, but is potentially preceded by an amorphous phase and/or nanoparticles of actually metastable bassanite ($CaSO_4{\cdot}0.5H_2O$),[65–67] which then aggregate in an ordered fashion (oriented attachment) and finally transform collectively into gypsum.[67] Further examples of inorganic materials forming transient precursor and intermediate phases can be found elsewhere.[68]

Another matter of debate is the actual mechanism whereby ACC transforms into crystalline phases. For example, when crystallizing vaterite under self-assembled monolayers, Pouget et al. observed assemblies of amorphous nanoparticles that over time developed crystalline domains within their volume (as indicated in step (j) in Figure 1).[28] Further evidence for such transformations in the solid state—however, not in contact with a solution—has recently been provided by a series of experiments in which ACC was crystallized by heating.[59] On the other hand, by using X-ray microscopy, Rieger et al. could show that ACC spheres dissolve completely, while crystalline calcium carbonate is formed somewhere else in the sample (see also Section 2.4.3).[69] This scenario is supported by a number of other studies.[36,44,70] The only conclusion we can draw so far is that both mechanisms are possible: solid-state phase trans-

formation within amorphous particles, as well as dissolution of these particles and a subsequent re-precipitation that is spatially decoupled from the position of the precursors. Furthermore, one could also imagine that the two mechanisms operate in parallel or successively, for example when a crystalline seed is initially formed by rearrangements in solid ACC and subsequently grows with units released through concurrent dissolution of the amorphous phase.

An alternative pathway to produce nanoparticles is growth by accretion of even smaller subunits (typically 1–3 nm). These primary particles are often assumed to form by classical nucleation, and may or may not already exhibit the crystalline structure of the final product (stages (f) and (g) in Figure 1). The aggregation of such building blocks can occur either by random or oriented attachment (stages (m) and (l) in Figure 1), thereby leading to superstructures with a greater or lesser degree of order.[71] A comprehensive overview on crystal architectures made from smaller subunits—so-called mesocrystals—and particle-based crystallization pathways in general can be found in the literature.[9,72]

2.4. Polymers Control the Formation of Nanoparticles

Allowing water-soluble polymers or polymeric template matrices to participate in the processes described in Sections 2.1–2.3 provides an additional degree of freedom for control over the outcome of particle formation and crystallization. This has clear potential for industrial applications as well as for understanding (and possibly mimicking) natural biomineralization.[2,7,9,73] Recent advances made in this promising field have been reviewed by Meldrum and Cölfen.[74] Some of the effects that will be described in the following are unexpected, such as the stabilization of amorphous liquid phases, while others may be expected, such as nucleation inhibition/promotion, templating, stabilization of nanoparticles, and modification of the crystal habit.

2.4.1. Polymer-Induced Liquid Precursors (PILPs) and Films

Even before the work of Faatz et al.,[34] liquid–liquid phase separation was experimentally verified by Gower and Odom,[75] who supersaturated a calcium carbonate solution in the presence of polymers, such as poly(aspartic acid), and observed liquid droplets large enough to be detectable under a light microscope. Originally, these species were named "polymer-induced liquid precursors" (PILPs) because it was assumed that they could only be formed with the help of polymers, which are thought to locally enrich calcium and/or carbonate ions in a condensed environment.[76] Meanwhile, it has become apparent that liquid $CaCO_3$ precursors may also occur in the absence of additives (see Section 2.2) and hence, the role of the polymers might rather be to stabilize this otherwise transient state than to actually induce it.[56] Another interesting recent finding in this area is that positively charged polymers can also sustain PILP phases.[77] In any case, the main advantage of liquidlike mineral precursors—from the point of view of crystal engineering and materials science—is the fact that they can be molded into basically any shape and thus yield complex non-equilibrium morphologies, which are eventually preserved by crystallization. The key task of the polymer is thus to delay solidification until structure formation is completed. Most notably, the PILP method seems to be very well suited for the preparation of thin films.[12] Similarly, porous matrices or template structures can readily be infiltrated by the liquid, thus giving relatively easy access to complex hybrid materials,[78] such as artificial bone.[79] More applications are discussed below. Details of the interaction between the dissolved polymers and the distinct calcium carbonate species in solution are still not well understood, but it is believed that the PILP phenomenon plays an essential role in biomineralization.[12,80]

2.4.2. Effects of Polymers during the Early Stages of Crystallization

Anionic polymers have been used for many years as additives to prevent scale formation, that is, the deposition of mineral particles on heat exchangers, in oil drilling holes, or in household appliances.[64,81] As evident from the information provided so far, it is difficult to identify the mode of action of these additives for the following reasons: 1) There are various possible precursor species that may all be affected or even controlled by the presence of polymers; since these structures have dimensions on the nanoscale they will not scatter light, hence will not appear turbid and thus evade standard tests used in industry.[82] 2) The interaction of, for example, polycarboxylates with divalent cations is complex and may involve the non-adjacent binding of ions to carboxylate groups for entropic reasons,[83,84] ion-induced polymer aggregation,[83,85] as well as ion-specific non-equilibrium effects.[86] 3) Polymers may bind to $CaCO_3$ ion pairs[87] or larger clusters[88] instead of simply sequestering calcium ions. 4) Polymer-ion, polymer-ion pairs, or polymer-cluster complexes may act as nucleating centers.[89] All this indicates that the mode of action of polymers at the level of precursors and initial particles is still not well understood and that further research is needed to enable a fully rational design of these polymers. A promising step in this direction has recently been made by the development of a quantitative, titration-based crystallization assay that allows different stages during the pre- and early post-nucleation phase to be probed.[90] This method has allowed a quite broad range of additives to be tested and classified with respect to effects such as ion complexation, (de)stabilization of prenucleation clusters, nucleation inhibition, and changes in the nature of the initially precipitated solid phase.[88,91] Even more insight can be gained when such experimental data are complemented by results from computer simulations, as has been done in a recent study on the influence of simple additives that differ only in the number of carboxylate groups.[92] One particularly interesting observation with respect to scale inhibition is that advanced antiscalants are able to effectively prevent nucleation at concentrations of only a few ppm, which is much less than actually needed for a mechanism based on simple ion sequestration. Here, one might argue that the key role of the scale inhibitors lies in their interaction with ion clusters and/or liquid droplets; for example, colloidal stabilization of these

species against aggregation and coalescence is a feasible scenario for polymer-induced nucleation inhibition at low additive concentrations.[30,88]

2.4.3. Stabilization of Nanoparticles

The above-described findings on the structures of nanoscale precursors in mineralization processes are of scientific relevance because of the rich behavior of precipitating systems and the many—still unsolved—questions occurring in this context. An interesting aspect of industrial relevance is the possibility to stabilize the intermediate nanoparticles, either amorphous or crystalline, against further ripening (stages (h) and (n) in Figure 1) by means of certain crystallization modifiers such as polymers or surfactants.[52,93] The amount of additive present during precipitation plays a decisive role in the evolution of the solid phase. In the case of calcium carbonate, it was shown that if the concentration of polymer is not sufficient to cover the surfaces of the nanoparticles efficiently, they will dissolve and crystals of mesoscopic size will form.[11] This effect is exemplarily illustrated in Figure 5 by means of a time sequence of X-ray microscopy

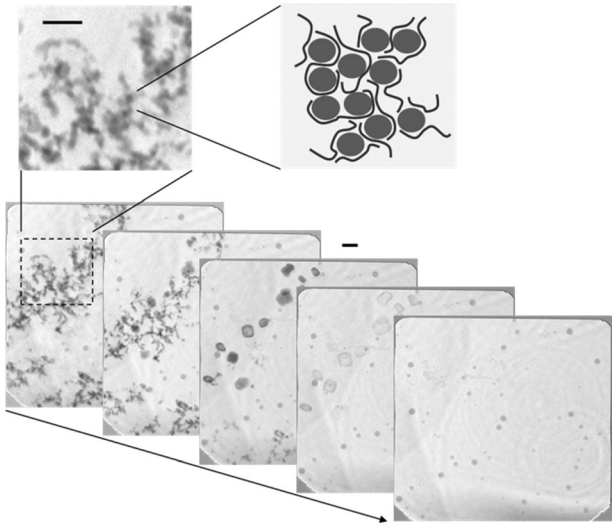

Figure 5. Direct in situ imaging of the progress of calcium carbonate crystallization by means of TXM. The first micrograph (left) was taken about ten minutes after mixing 0.01 M solutions of $CaCl_2$ and Na_2CO_3 in the presence of 200 ppm polycarboxylate. The five micrographs cover a time interval of four minutes. Scale bars: 1 μm. Adapted from Ref. [11] with permission from the Royal Society of Chemistry, Copyright 2007.

(TXM) images recorded directly from solution. First, amorphous nanoparticles embedded in a network of polymers are observed (see enlargement of the left panel in Figure 5). In the second micrograph, these particles have started to dissolve and objects with dimensions of about one micrometer have appeared. In view of the regular shape of these objects (which becomes even clearer in the third picture), it is assumed that the calcium and carbonate ions released during dissolution of the nanospheres re-precipitate as crystalline particles in the vicinity. However, these crystals re-dissolve (images 4 and 5 in Figure 5), which suggests that they are composed of a metastable phase. This indicates that either one of the less stable modifications of calcium carbonate is formed and stabilized against further growth by adsorbing polymers, or that the crystal itself is destabilized by the presence of—possibly incorporated—polymers. Since there must be a sink for the ions released upon dissolution of the observed structures, we conclude that more stable crystals must have formed during the process outside the area observed with the X-ray microscope.

More information about the role of the polymer during the formation of the solid phase can be gained by means of calcium activity measurements performed with ion-selective electrodes. In this way, the amount of polymer necessary to stabilize the particles could be determined quantitatively and related to the surface area of the particles. Furthermore, it could be shown that part of the polymer is trapped inside the particles while another fraction is still active in the solution, interacting with free ions or ion clusters.[11]

2.5. Industrial Relevance—Making Use of Precursor Structures

The occurrence of multiple precursor and intermediate stages in the crystallization of solid materials—as well as the properties and interactions of these distinct species in solution—has numerous potentially important implications for industrial processes, some of which will be briefly outlined in the following. We do not seek to be comprehensive in this context, but rather intend to give selected examples that we find particularly interesting. One of these refers to the discovery that amorphous minerals, both biogenic and synthetic, can apparently exist in different structural forms.[49,57,60,61] Even more intriguingly, it seems as if the short-range order in amorphous particles (and perhaps even in prenucleation species) can to some extent prescribe the pathway to the thermodynamically more stable crystalline phases, that is, polymorph selection might already be encoded in these early precursors.[25,60] This field of research is still in its infancy, but one may speculate whether it will be possible to control the polymorphism of pharmaceuticals or pigments by influencing the protostructure of their amorphous state—which in turn could be accomplished by adjusting the process conditions or introducing suitable additives.

The distinct ability of PILP phases to form mineral/polymer thin films has clear potential for the fabrication of hybrid coatings.[12] In addition, the PILP approach can also be used to generate mineral fibers.[94] This becomes even more attractive when considering that the phenomenon is not limited to calcium carbonate. For example, it has been shown that uniform and smooth films of zinc oxide can be obtained by directing mineral formation through an intermediate amorphous phase stabilized by poly(vinylpyrrolidone).[95] Furthermore, it has recently been reported that polymer-induced liquid precursors may also occur in the crystallization of organic compounds:[96] in the presence of poly(acrylic acid), the amino acid lysine formed PILP droplets that coalesced into spherulitic thin films, which later recrystallized to give mesocrystalline mosaic patterns. However, at the

moment it has not yet been explored to what extent strategies such as this could provide coatings and fibers with properties superior to those achieved in established production processes.[97]

From a materials science perspective, another feasible way to benefit from transient crystallization precursors is to capture amorphous nanoparticles directly during precipitation by incorporation into an organic matrix, thus yielding hybrid nanostructures in a simple one-step synthesis. This has been realized by Oaki et al., who prepared crack-free transparent composite materials consisting of small ACC grains, about 2 nm in size, embedded in a framework of poly(acrylic acid).[98] Interestingly, these structures were found to be capable of including a variety of functional organic molecules and inorganic particles, which clearly broadens the scope of possible applications. In a similar approach, Gebauer et al. synthesized composites of nanocrystalline cellulose and amorphous calcium carbonate, which showed promising optical and mechanical properties and hence may serve as multifunctional biodegradable hybrid materials.[99]

As already discussed in the previous section, the use of polymers to prevent scaling is well-established in both household and industrial applications.[64,81] Even though the precise mode of action of these additives at the nanoscale is not yet fully understood, the growing interest in the interaction between polyelectrolytes and inorganic precursor species over the past years raises hope that progress in this field will be faster in the future. Perhaps, the insight gained from such studies may at some point allow for a more rational development of even better additives (more selective, more efficient) for scale inhibition as well as for the fabrication and/or processing of hybrid and construction materials (which will be addressed in more detail below).

Stabilizing intermediate nanoparticles with the aid of suitable additives furthermore represents a valuable concept to exploit the specific size-dependence of properties inherent to materials applied as pigments, ion exchangers, fillers, and others. One example in this context is the development of a production process for nanosized zinc oxide particles for transparent UV protection.[100] This was achieved by precipitation from solutions containing zinc acetate (0.2 M), sodium hydroxide (0.4 M), and, for example, poly(aspartic acid) (4 $g L^{-1}$). Under these conditions, the formed ZnO nanoparticles (ca. 50 nm in diameter; Figure 6) are stabilized by the polymer and kept in a dispersed state.

By using a similar concept, stable (nano)particles of vaterite can be obtained in the presence of additives such as poly(vinylsulfonic acid),[101] or by conducting the precipitation in membrane reactors in the presence of alcohols.[102] Moreover, Nudelman et al. achieved stabilized ACC particles with an average size of 50 nm by protecting them against crystallization with poly(aspartic acid).[103] In the case of calcium sulfate, the kinetic stability of both the amorphous and the hemihydrate phase could be improved by the addition of polymers such as poly(acrylic acid) or poly(styrene sulfonate),[104] as well as small molecules such as citrate.[66] This is particularly interesting because bassanite, a widely applied binder in cements and mortars, is currently produced by heating gypsum, and an additive-based process at room temperature might hence represent a cost-efficient alternative synthesis strategy. Despite all these examples of successful nanoparticle stabilization, our understanding of how to select the right polymer for a given inorganic system is still only slowly evolving.

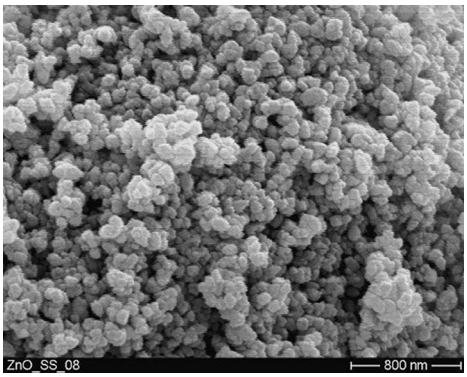

Figure 6. SEM image of ZnO nanoparticles obtained by precipitation in the presence of poly(aspartic acid) (unpublished data).

3. The Nanostructure of Cement

3.1. Industrial Relevance of Cement and Perspective

Concrete is a construction material consisting of cement, sand, gravel, and water. It is by far the largest scale man-made material when measured by total weight. Although known for thousands of years, concrete still offers plenty of opportunities to innovative industries. One of these is to use more sustainable raw materials in cement production (without any detriment to the final properties) to reduce the CO_2 emissions arising from concrete. As a consequence of the huge volume produced each year (ca. 8 billion m^3), concrete is responsible for about 7% of the anthropogenic CO_2 emissions. Reducing these emissions poses one of the biggest challenges in terms of sustainability.[105] Two approaches have been identified to address this issue. The first one is based on the optimization of technologies associated with concrete production, such as burning or grinding, the switch to biomass fuels, and the use of secondary cementitious materials which are either by-products of other processes or some readily accessible natural materials. The second approach—related to the topic of this Review and further explained below—is to modify the intrinsic mechanical properties of concrete through the design of more efficient nano-, micro-, and mesostructures to obtain more strength with less reactive material. In the past, the emergence of highly efficient organic plasticizers enabled the development of ultrahigh-performance concretes (UHPCs) with compressive strengths above 200 MPa, which could still flow despite their very high solid content. The performance of UHPC was ascribed to the geometrical optimization of the packing of all the elements constituting the concrete. This technique represents a typical top-down approach to drastically reduce the porosity and thus to increase the mechanical strength.[106]

For roughly a decade, chemists and physicists have also scrutinized the nanoscale to improve the properties of cement and related materials. This time, bottom-up approaches are being investigated. The aim is to "build" the properties of concrete materials from its basic constituent units (atoms) to form macroscopic structures,[107] where one of the targets is to reduce creep.[108] Substantial effort is still required to devise the right molecules or additives for obtaining a cement structure at the nanoscale with the desired enhanced performance. The success of this endeavor depends on whether it is possible to bridge the gap of scientific understanding at the various length scales. Nevertheless, some progress has been made with respect to controlling the precipitation of calcium silicate hydrate (C-S-H), which is the most important phase of hydrated cement and which will be discussed in the following section.

3.2. The C-S-H Phase: The Nanoglue of Cement

Cement is a complex, nanostructured multiphasic material mostly composed of tricalcium silicate (C_3S), dicalcium silicate (C_2S), anhydrous aluminate phases (C_3A and C_4AF),[109] and sulfate carriers (essentially bassanite and anhydrite). All these phases dissolve in contact with water and produce various species, the cement hydrates. The key reactions are the dissolution of C_3A and C_4AF, which rapidly gives ettringite-type phases, and above all the hydration of C_3S and C_2S, which lead to the precipitation of C-S-H phases and portlandite ($Ca(OH)_2$). The typical evolution of the composition of ordinary cement over three years is shown in Figure 7,[110] while the microstructure developed after 24 h of hydration is shown in Figure 8. The cohesion of cement and its mechanical properties are mainly due to C-S-H, as will be explained in detail below.

Despite its omnipresence in daily life, the basic constitution—that is, the crystal structure—of C-S-H in cement pastes is not yet fully resolved and still debated in the scientific community. There is some agreement that the C-S-H structure is close to tobermorite-11 Å, a natural calcium silicate consisting of layers that are composed of calcium atoms sandwiched between parallel silicate chains. While the silicate chains in the tobermorite structure are infinite, C-S-H grains typically contain shorter oligomers. Figure 8d shows one of the likely C-S-H structures, which contains dimeric silicates exclusively, as proposed by Richardson.[111] As a consequence of the lack of conclusive experimental evidence, the most recent attempts to elucidate the crystal structure of C-S-H are based on computer modeling[112] and still subject to controversy.[113] Resolving the structure of C-S-H is of prime importance, since the data are used[107] and/or could be used in the future for advanced meso- or macroscopic models to assess the final mechanical properties and thus the durability of cementitious materials. In addition, a better knowledge of the C-S-H structure and of its ability to accommodate, for example, aluminum ions could enhance the sustainability of concrete[114] and also lead to a better thermodynamic model, which is a necessary requirement for prediction of the long-term service life of cement waste materials.[115]

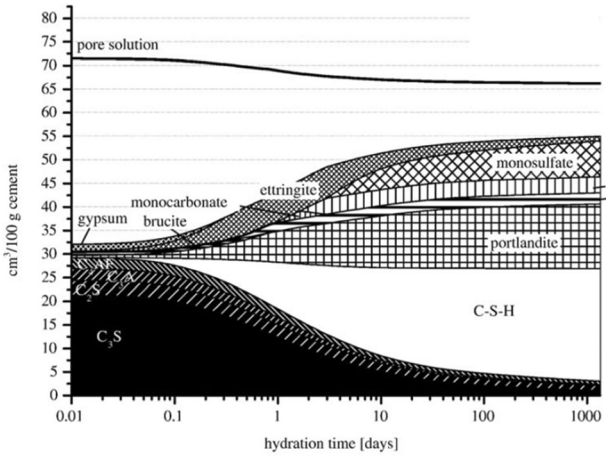

Figure 7. Evolution of the composition of typical ordinary cement upon hydration (when 1 g of cement is mixed with 0.4 g of water). Reproduced from Ref. [110] with permission from Elsevier, Copyright 2008.

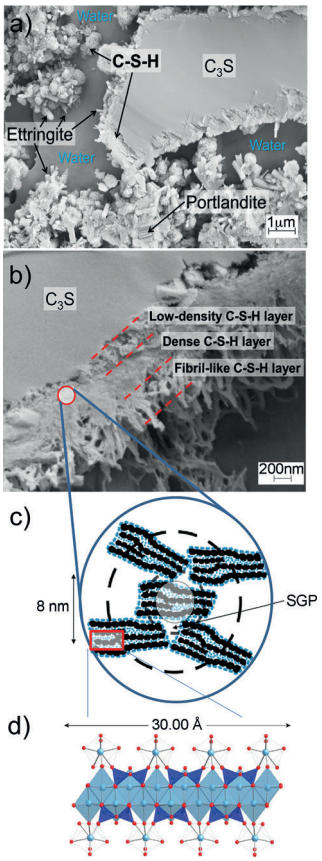

Figure 8. a,b) Cryo-SEM images of cement with the same composition as in Figure 7 and observed after one day. The main hydration products are clearly visible (unpublished work; see Ref. [117] for more information on sample preparation). c) Arrangement of C-S-H platelets leading to nanoporosity according to Jennings' colloidal model (SGP stands for small gel pore). Reproduced from Ref. [116] with permission from Elsevier, Copyright 2008. d) Proposed C-S-H structure with a calcium-to-silicon ratio of 1.5:1. Reproduced from Ref. [111] with permission from Elsevier, Copyright 2004.

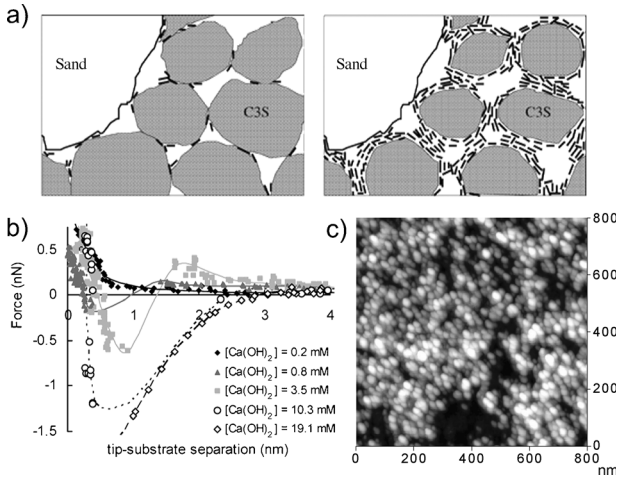

Figure 9. a) Sketch illustrating the role played by C-S-H nanoplatelets forming around the C_3S grains in the development of a cohesive nano- and microstructure. At very early stages, the grains are connected only at a few points, thereby resulting in a weak network. Upon hydration, the C-S-H platelets continue to precipitate and enlarge the contact surface area between the grains, thus strengthening the network. Reprinted from Ref. [121] with permission from the American Chemical Society, Copyright 2005. b) Force as a function of distance between C-S-H surfaces as measured by atomic force microscopy at different concentrations of calcium hydroxide in solution. Above 1 mM $Ca(OH)_2$, the force switches from repulsive to attractive because of ion–ion correlation effects. Reprinted from Ref. [118] with permission from the American Chemical Society, Copyright 2005. c) C-S-H nanoparticles precipitated onto a cement surface and visualized by AFM. Reproduced from Ref. [113e] with permission from Elsevier, Copyright 2004.

The C-S-H particles are nanoplatelets with dimensions in the range of 50 nm (Figure 9c)[116] or fibril-like structures[111,113] (Figure 8b);[117] they form within a gel around the C_3S grains. The mechanical properties of cementitious materials are dependent on C-S-H for two reasons. First, C-S-H precipitates in the form of small interlocked crystallites, that is, with a high specific surface area, which results in a large contact area between individuals. Second, there is strong attraction between the C-S-H surfaces at the typical pH value of cement (ca. 13) and in the presence of calcium ions (Figure 9b).[118] These electrostatic forces are caused by the high surface charge density of C-S-H ($4.8\,e^{-}\,nm^{-2}$)[119] resulting from the deprotonation of silanol groups at the surface under alkaline conditions. In the presence of divalent cations, such as Ca^{2+}, this negative charge density leads to strong ion–ion correlation effects.[120]

One characteristic feature of these forces is their insensitivity to the composition of the cement pore solution, which may vary substantially depending on the local raw materials used for production. Despite an ionic strength of up to 1 M, the force remains attractive as long as the pH value is high enough and the calcium concentration exceeds about 2 mM. On the other hand, the strength of these forces is also responsible for the irreversible aggregation of the C-S-H particles, which causes a more or less disordered assembly of these nanobricks (Figures 8c and 9a);[116,121] consequently, the formed nanopores exhibit a certain size distribution, which can be measured by ^1H NMR relaxometry during hydration or by scattering techniques.[122]

The formation of a disordered inorganic network constituted of layered nanoplatelets is a challenge for chemists interested in designing cementitious materials with superior mechanical properties. First attempts to achieve this on the basis of polymer–cement composites were made in the 1920s, and resulted in improved flexibility and adhesion, as well as good abrasion and chemical resistances.[123] Typically, the cement matrix and polymer are mixed on the micrometer scale. The addition of high-molecular-weight water-soluble polymers, such as poly(vinylpyrrolidone) or poly(vinyl alcohol), enhances the toughness of cement pastes by increasing the energy necessary to initiate cracks and by impeding crack propagation through polymer–cement bridges.[124] Although many examples demonstrate the good performance of composite materials based on hybridization at the micrometer level,[125] even better mechanical properties could be expected when the cement hydrates and organic compounds are intimately combined at the nanoscale. For example, it is possible to insert polymers between distinct C-S-H crystallites[126] or to form organosilicate hybrids.[127] Franceschini et al. showed that the Young's modulus of silane-based C-S-H hybrid materials almost doubled with the incorporation of 2% silanated polymers.[126] In another study, the addition of poly(ethylene glycol) or poly(acrylic acid) increased the degree of polymerization of the silicate chains present in C-S-H.[128] The authors aimed to improve the chemical resistance, and thus the durability of the material, but did not provide experimental evidence to support this was achieved. Furthermore, as the C-S-H structure exhibits some similarities with clays (smectites)—in which the intercalation of polymers at the atomic level leads to the formation of nanocomposites with excellent mechanical properties[129]—it was expected that this concept can be transferred to C-S-H. However, C-S-H cannot swell like smectites, and it is therefore impossible to intercalate polymers in its layered crystal structure,[130] although other studies seem to provide some supportive evidence.[131] Thus, the smallest scale realized to date for the hybridization of C-S-H and polymers is still limited to the size of the C-S-H crystallites. Nevertheless, there is evidence that other cement hydrates, namely calcium hydroaluminates (the so-called AFm phases), can form layered polymer–inorganic structures even at a smaller scale.[132] This may open a new window in the field of cementitious composites based on aluminum-rich raw materials or for aluminous cement.

3.3. C-S-H Nucleation and Prenucleation Stages

The mechanisms underlying the nucleation of C-S-H particles are still not well understood. So far, the only information about nucleation in real systems derives from time-dependent data of the degree of cement (or C_3S) hydration, which were analyzed using different models—with some cases of disagreement.[117,133] Unsurprisingly, all the models suggest that the nucleation step plays an important role in the hydration kinetics, at least during the very early

stages, thus affecting the mechanical properties from the onset of setting. This insight is crucial for improving the cost efficiency of industrial concrete production, especially in the precast industry. Understanding C-S-H nucleation is essential for developing strategies to, first, accelerate the hydration process and, second, gain better control over cement reactivity, a key aspect in the concrete industry.

When discussing the complexity of both nucleation and prenucleation stages, it is of course important to know the final crystal structure, which in the case of C-S-H is still under debate, as pointed out above. Experimental work by Garrault-Gauffinet and Nonat allowed the estimation of the interfacial energy of the critical C-S-H nucleus to be about 10–15 $mJ\,m^{-2}$,[134] a relatively small value compared to other crystals. This finding indicates that C-S-H should already precipitate at low supersaturation. The elementary steps occurring before and after the formation of this critical nucleus are still obscure; in particular, it is not known whether a sequence of phase transitions, as discussed for $CaCO_3$ in Section 2, has to be considered. However, recent studies indicate that negatively charged silicate chains (oligomers) are first formed by condensation of monomeric species under the charge-screening influence of Ca^{2+} counterions, and subsequently transform into a C-S-H phase.[135] Such catalytic behavior of calcium ions was already proposed in the context of the formation of silico-calco-alkaline gels.[136]

Despite the relatively poor knowledge about the mechanisms underlying C-S-H nucleation (as compared to the calcium carbonate case, for example), concrete and mortar formulators have been using organic additives to retard the nucleation of C-S-H in cement pastes for a long time.[137] The main purpose of this effect is to provide a sufficiently long workability period to transport the formulated concrete from the plant to the job site. It is important to note that modification of the nucleation may not only have consequences for the early hydration and strength of cement,[133a] but also for the properties of the aged concrete.[138] The study by Garrault and Nonat, who investigated C-S-H nucleation on a more systematic basis,[139] undoubtedly demonstrates that the amount of generated nuclei influences cement hydration over several days. Indeed, the porosity, thickness, and structure of the dense C-S-H layer (Figure 8b) developing around the cement particles can be determined by nucleation. For example, a loosely packed and thus more permeable C-S-H layer will enhance subsequent hydration if the process is limited by the diffusion of ions at that time.[140] More generally speaking, all current hydration models agree on the fact that the early nano- and microstructure of cement pastes is strongly influenced by nucleation and its accompanying structural evolution. On the other hand, the compressive strength after 28 days,[141] which represents the key reference value of concrete, is not significantly affected by the presence of additives interfering with nucleation. In this regard, we can conclude that with our current knowledge it is possible to accelerate the development of the nano- and microstructure in the early stages, but it is still challenging to modify the final microstructure and properties of concrete.

3.4. C-S-H Suspensions—Control of Aggregation

As a consequence of the attractive forces mentioned in Section 3.2 (Figure 9b), C-S-H particles are prone to aggregation and then become difficult to manipulate. It is therefore desirable to prevent uncontrolled particle aggregation and achieve stable colloidal suspensions, which might help to produce modified C-S-H-based materials with improved properties. An interesting example is to use suspensions of C-S-H seeds as hardening accelerators for concrete. The seeding technique, well-established in many other fields, has been known for a long time in concrete applications,[142] but has been explored only with limited success until recently.[133a,143] However, a breakthrough has been achieved, and colloidally stable seed suspensions can be synthesized. In one particular example, hydrophilic phosphated comb polymers control the aggregation of C-S-H particles in such a way that the disclike particles will still aggregate, but preferentially in an edge-to-edge orientation.[144] This yields open fractal structures of C-S-H platelets, in which the particles are stabilized to such an extent that compact aggregates are prevented (Figure 10).

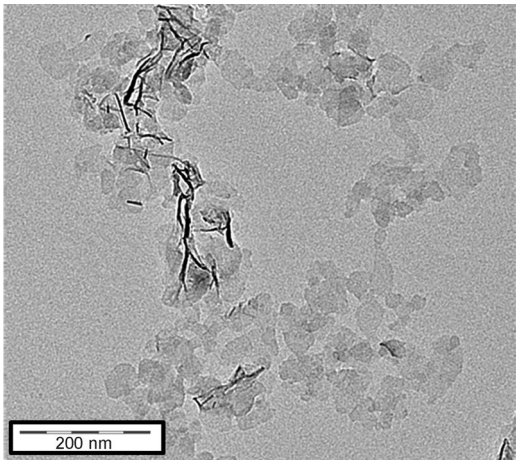

Figure 10. TEM image of an aggregate formed by C-S-H platelets that were synthesized in the presence of a comb polymer. The particles are only 1.4 nm thick and are mostly connected edge-to-edge. Therefore, they exhibit large specific areas and can be used as seeding substrates. Reproduced from Ref. [144] with permission from the Royal Society of Chemistry, Copyright 2013.

The obtained suspensions show unique properties that are not displayed by either perfectly dispersed nanoparticles or dense aggregates. In particular, if the fractal dimension is low, C-S-H aggregates exhibit an open texture with high surface area, which is beneficial for application as seeding additives.[145] This finding also emphasizes that aggregates of nanoparticles do not necessarily need to be ordered in a regular manner to become relevant for industrial processes. Indeed, fractal objects are a class of disordered structures with interesting properties in many respects; for example, corresponding fumed silica materials can be used as thickening agents, abrasives, or desiccants. Furthermore, fractal structures can be tuned by orienting the particles in an

external field (e.g. magneto-rheological fluids),[146] and have found applications in the pharmaceutical sciences[147] as well as for analytical techniques.[148]

Apart from the controlled aggregation into fractal clusters as described above, it is also possible to stabilize C-S-H particles by the addition of adsorbing high-molecular-weight polymers. For example, comb-type copolymers of acrylic acid and poly(ethylene glycol) macromonomers protect single C-S-H particles against aggregation.[144] An important feature of these polymers is that they contain groups which promote adsorption (e.g. carboxylate functionalities) as well as neutral hydrophilic segments that provide steric repulsion between the C-S-H platelets.[149] The interactions between inorganic surfaces and polymers can be complex and the range of (co-)polymers available to achieve specific effects is large. Phage display has proven to be a valuable tool to identify the polymer which has the most suitable chemical motif and/or best sequence of functional groups for binding to a given substrate.[150] This technique is mostly used for the high-throughput screening of protein–protein interactions, but also for protein–substrate interactions. Applied to C-S-H, it was shown that peptides including amino acids with anionic functionalities and proton donors can specifically adsorb on C-S-H at pH 13, that is, the typical conditions found in cement.[151]

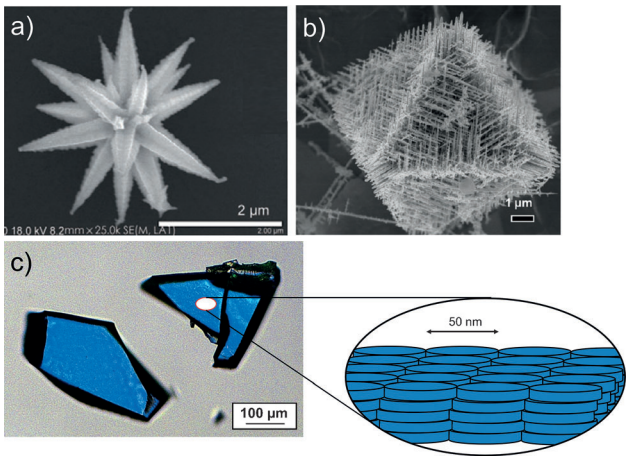

Figure 11. a) FESEM image of a gold "mesoflower" showing excellent (near-)infrared absorption properties, which might be used for optical filters. Reprinted from Ref. [153] with permission from Springer, Copyright 2009. b) Cu_2O nanowire based mesocrystalline octahedron exhibiting superior gas-sensing performance. Reproduced from Ref. [154] with permission from the American Chemical Society, Copyright 2012. c) Large C-S-H mesocrystals observed by polarized optical microscopy (image courtesy of H. Cölfen). The crystals consist of single C-S-H platelets, about 50 nm in diameter. Both pieces exhibit uniform color when viewed under crossed polarizers, which means that all the particles are aligned in the same direction.[135]

3.5. Organization of C-S-H Particles into Mesocrystalline Structures

Inspired by nature's ingenuity to design hybrid materials of seemingly unlimited structural complexity in living organisms,[7] scientists have undertaken many attempts to organize matter into more and more intricate systems, as for example in supramolecular chemistry[152] or hybrid nanomaterials research.[1] One general concept often used to generate elaborate crystalline structures in the laboratory is to prepare so-called mesocrystals,[9,72,153] as already mentioned in Section 2.3. These architectures look (and scatter) like single crystals even though they are composed of nanoparticles, and are not all perfectly aligned. Moreover, mesocrystals can exhibit very different behavior from their constituting nanocrystals, sometimes outperforming their corresponding reference materials. Some of the properties they display are very interesting, such as anomalous magnetism, superior strength, collective vibrations, high internal porosity, or enhanced stability. Some illustrative examples of superstructures made from nanocrystals are reproduced in Figure 11. All of them are distinguished by one specific property that renders their use as new materials attractive.[153,154] By using mesocrystals synthesized in vitro, it is now possible to bridge the field of biomaterials with that of functional materials including new sensors,[154] photonic devices,[155] catalysts,[156] and others.[9,72,157]

The motivation to synthesize C-S-H-based mesocrystals is the hope to remedy the poor ductility of concrete. The attractive forces between C-S-H crystallites are very short-ranged, which has a negative effect on the tensile strength. As in the case of many hybrid materials found in nature where fragile minerals are one of the constituents, the addition of polymers lends ductility to the inorganic structure.[158] The potential of this approach is highlighted in a very recent study on the crystallization of calcium carbonate in the presence of a silicatein protein, which gave calcite spicules exhibiting outstanding flexibility and unprecedented elastic bending behavior, completely distinct from the properties of the pure mineral and even outperforming natural spicules.[159,160] It is tempting to draw a parallel with C-S-H, but applying such concepts to the nanobricks of cement requires the identification of suitable organic components. For example, C-S-H nanoplatelets can be stabilized and assembled into large mesocrystals with the aid of hydrophilic block copolymers, as shown in Figure 11c.[135,161] These hybrid structures show mechanical properties superior to those of ordinary cements, especially in terms of flexibility, and thus represent promising candidates for construction materials in earthquake-prone areas, since the brittle character of concrete may be drastically reduced.

Most of the properties of concrete are closely related to the nanostructured C-S-H network. A profound understanding of C-S-H formation, ranging from initial nucleation event(s) over the crystal structure to the way the crystallites pack together, will ultimately permit the design of stronger and more sustainable cementitious materials. For example, the incorporation of more aluminum ions or alkali ions into the crystal structure will allow the use of more supplementary matter during the clinkering process, and hence will improve the sustainability.[162] For a given composition, the understanding and subsequent design of a cement matrix on all length scales appears to be the only route toward "greener" concrete materials.[163] As a result of the complexity of the material, the next breakthrough developments are expected

to be strongly supported by multiscale modeling approaches capable of addressing all relevant aspects.[164] Polymers offer the possibility to modify the intrinsic properties of concrete, and some promising strategies have already been identified. The next, but still ambitious, step is to transfer the laboratory-scale insight to the mass-production of concrete, which remains heavily constrained by cost considerations.

4. Conclusion

Solute clustering, liquid–liquid phase separation, nucleation, growth and ripening, polymorphic transformations, particle aggregation, and superstructure formation are stages involved in many precipitation and crystallization processes. Understanding all these complex and often coupled steps is crucial to shed light on biomineralization phenomena, but it also bears fundamental relevance for industry, where one promising way to provide even better materials is to mimic the self-organization principles mastered by nature. There is a steady need for better and more sustainable materials to address important contemporary challenges. However, the performance of all solid materials depends on structural features at various hierarchical levels, that is, from the nano- over the meso- up to the macroscale. Therefore, the improvement of existing—and design of future—high-performing materials essentially relies on a profound understanding of structure–property relationships at all relevant length scales. An ultimate goal would be the ability to predict interactions between, preferably simple, starting compounds and "program" their self-assembly into more complex matter, that is, a rational concept of bottom-up approaches to materials with specific structures and hence properties. There are indeed some model systems where this has partially been achieved,[165] but clearly much work remains to be done to gain full control over crystallization.

Our knowledge about the materials science behind many macroscopic phenomena is still limited, especially at the nanoscale—despite the fact that some of these materials have already been used on a large scale for decades or even centuries, as cement can attest. There are still many key questions left unanswered—especially those related to the composition, structure, and properties of precursors occurring during the solidification of materials in crystallization reactions. One of the main hurdles lies in the difficulty to experimentally access the time and length scales at which nucleation processes take place, that is, to design techniques that provide micro- to millisecond temporal and (sub-)nanometer spatial resolution. As an alternative, or rather a complementary approach, much effort is being invested in the development of more powerful modeling tools to probe these stages. Although there is still a long way to go to finally achieve true multiscale simulations of dynamic phenomena, impressive progress has been made in recent years. We are convinced that at least some of the open questions addressed in this Review will find satisfying answers in the near future.

Received: March 4, 2014
Published online: August 26, 2014

[1] a) L. Cademartiri, G. A. Ozin, *Concepts of Nanochemistry*, Wiley-VCH, Weinheim, **2009**; b) *Advanced Nanomaterials* (Eds.: K. E. Geckeler, H. Nishide), Wiley-VCH, Weinheim, **2009**; c) H. F. Tibbals, *Medical Nanotechnology and Nanomedicine*, CRC, Boca Raton, **2011**; d) W. Pompe, G. Rödel, H. J. Weiss, M. Mertig, *Bio-Nanomaterials*, Wiley-VCH, Weinheim, **2013**; e) *Nanotechnology for the Energy Challenge*, *2nd ed.* (Ed.: J. Garcia-Martinez), Wiley-VCH, Weinheim, **2013**; f) *Nanomaterials in Catalysis* (Eds.: P. Serp, K. Philippot), Wiley-VCH, Weinheim, **2013**;.

[2] a) F. Nudelman, K. Pieterse, A. George, P. H. H. Bomans, H. Friedrich, L. J. Brylka, P. A. J. Hilbers, G. de With, N. A. J. M. Sommerdijk, *Nat. Mater.* **2010**, *9*, 1004 – 1009; b) P. A. Fang, J. F. Conway, H. C. Margolis, J. P. Simmer, E. Beniash, *Proc. Natl. Acad. Sci. USA* **2011**, *108*, 14097 – 14102.

[3] ISO/TS 80004-1:2010(E).

[4] A. S. Myerson, *Handbook of industrial crystallization*, Butterworth-Heinemann, Woburn, **2002**.

[5] R. J. Davey, S. L. M. Schroeder, J. H. ter Horst, *Angew. Chem.* **2013**, *125*, 2220 – 2234; *Angew. Chem. Int. Ed.* **2013**, *52*, 2166 – 2179.

[6] F. Otálora, J. M. García-Ruiz, *Chem. Soc. Rev.* **2014**, *43*, 2013 – 2026.

[7] a) H. Lowenstam, S. Weiner, *On Biomineralization*, Oxford University Press, New York, **1989**; b) S. Mann, *Biomineralization: principles and concepts in bioinorganic materials chemistry*, Oxford University Press, New York, **2001**; c) L. Addadi, S. Weiner, *Angew. Chem.* **1992**, *104*, 159 – 176; *Angew. Chem. Int. Ed. Engl.* **1992**, *31*, 153 – 169; d) S. Weiner, L. Addadi, *Annu. Rev. Mater. Res.* **2011**, *41*, 21 – 40.

[8] a) A. A. Chernov, *Modern Crystallography III: Crystal Growth*, Springer, Berlin, **1984**; b) O. Söhnel, J. Garside, *Precipitation*, Butterworth-Heinemann, Oxford, **1992**; c) J. W. Mullin, *Crystallization*, Butterworth-Heinemann, Oxford, **1997**.

[9] H. Cölfen, M. Antonietti, *Mesocrystals and non-classical crystallization*, Wiley, Chichester, **2008**.

[10] A. V. Radha, T. Z. Forbes, C. E. Killian, P. U. P. A. Gilbert, A. Navrotsky, *Proc. Natl. Acad. Sci. USA* **2010**, *107*, 16438 – 16443.

[11] J. Rieger, T. Frechen, G. Cox, W. Heckmann, C. Schmidt, J. Thieme, *Faraday Discuss.* **2007**, *136*, 265 – 277.

[12] L. B. Gower, *Chem. Rev.* **2008**, *108*, 4551 – 4627.

[13] a) M. Volmer, A. Weber, *Z. Phys. Chem.* **1925**, *119*, 277 – 301; b) R. Becker, W. Döring, *Ann. Phys.* **1935**, *416*, 719 – 752.

[14] a) K. F. Kelton, A. L. Greer, *Nucleation in Condensed Matter*, Elsevier, Amsterdam, **2010**; b) D. Kashchiev, *Nucleation: Basic theory with applications*, Butterworth-Heinemann, Oxford, **2000**; c) J. J. De Yoreo, P. Vekilov, *Rev. Mineral. Geochem.* **2003**, *54*, 57 – 93.

[15] P. G. Vekilov, *Nanoscale* **2010**, *2*, 2346 – 2357.

[16] A. Navrotsky, *Proc. Natl. Acad. Sci. USA* **2004**, *101*, 12096 – 12101.

[17] T. Z. Forbes, A. V. Radha, A. Navrotsky, *Geochim. Cosmochim. Acta* **2011**, *75*, 7893 – 7905.

[18] P. Raiteri, J. D. Gale, *J. Am. Chem. Soc.* **2010**, *132*, 17623 – 17634.

[19] W. Ostwald, *Z. Phys. Chem.* **1897**, *22*, 289 – 330.

[20] Q. Hu, M. H. Nielsen, C. L. Freeman, L. M. Hamm, J. Tao, J. R. I. Lee, T. Y. J. Han, U. Becker, J. H. Harding, P. M. Dove, J. J. De Yoreo, *Faraday Discuss.* **2012**, *159*, 509 – 523.

[21] D. Erdemir, A. Y. Lee, A. S. Myerson, *Acc. Chem. Res.* **2009**, *42*, 621 – 629.

[22] R. P. Sear, *Int. Mater. Rev.* **2012**, *57*, 328 – 356.

[23] a) M. A. Larson, J. Garside, *Chem. Eng. Sci.* **1986**, *41*, 1285 – 1289; b) A. S. Myerson, P. Y. Lo, *J. Cryst. Growth* **1991**, *110*, 26 – 33.

[24] a) J. R. Clarkson, T. J. Price, C. J. Adams, *Faraday Trans.* **1992**, *88*, 243 – 249; b) J. Y. Gal, J. C. Bollinger, H. Tolosa, N. Gache, *Talanta* **1996**, *43*, 1497 – 1509.
[25] D. Gebauer, A. Völkel, H. Cölfen, *Science* **2008**, *322*, 1819 – 1822.
[26] D. Gebauer, H. Cölfen, *Nano Today* **2011**, *6*, 564 – 584.
[27] D. Gebauer, M. Kellermeier, J. D. Gale, L. Bergström, H. Cölfen, *Chem. Soc. Rev.* **2014**, *43*, 2348 – 2371.
[28] E. M. Pouget, P. H. H. Bomans, J. A. C. M. Goos, P. M. Frederik, G. de With, N. A. J. M. Sommerdijk, *Science* **2009**, *323*, 1455 – 1458.
[29] R. Demichelis, P. Raiteri, J. D. Gale, D. Quigley, D. Gebauer, *Nat. Commun.* **2011**, *2*, 590.
[30] M. Kellermeier, D. Gebauer, E. Melero-Garcia, M. Drechsler, Y. Talmon, L. Kienle, H. Cölfen, J. M. Garcia-Ruiz, W. Kunz, *Adv. Funct. Mater.* **2012**, *22*, 4301 – 4311.
[31] W. J. E. M. Habraken, J. Tao, L. J. Brylka, H. Friedrich, L. Bertinetti, A. S. Schenk, A. Verch, V. Dmitrovic, P. H. H. Bomans, P. M. Frederik, J. Laven, P. van der Schoot, B. Aichmayer, G. de With, J. J. De Yoreo, N. A. J. M. Sommerdijk, *Nat. Commun.* **2013**, *4*, 1507.
[32] M. Kellermeier, R. Rosenberg, A. Moise, U. Anders, M. Przybylski, H. Cölfen, *Faraday Discuss.* **2012**, *159*, 23 – 45.
[33] M. Kellermeier, A. Picker, A. Kempter, H. Cölfen, D. Gebauer, *Adv. Mater.* **2014**, *26*, 752 – 757.
[34] M. Faatz, F. Gröhn, G. Wegner, *Adv. Mater.* **2004**, *16*, 996 – 1000.
[35] a) D. Pontoni, J. Bolze, N. Dingenouts, T. Narayanan, M. Ballauff, *J. Phys. Chem. B* **2003**, *107*, 5123 – 5125; b) M. Faatz, W. Cheng, G. Wegner, G. Fytas, R. S. Penciu, E. N. Economou, *Langmuir* **2005**, *21*, 6666 – 6668; c) J. Liu, J. Rieger, K. Huber, *Langmuir* **2008**, *24*, 8262 – 8271.
[36] a) S. E. Wolf, J. Leiterer, M. Kappl, F. Emmerling, W. Tremel, *J. Am. Chem. Soc.* **2008**, *130*, 12342 – 12347; b) S. E. Wolf, L. Müller, R. Barrea, C. J. Kampf, J. Leiterer, U. Panne, T. Hoffmann, F. Emmerling, W. Tremel, *Nanoscale* **2011**, *3*, 1158 – 1165.
[37] M. A. Bewernitz, D. Gebauer, J. R. Long, H. Cölfen, L. B. Gower, *Faraday Discuss.* **2012**, *159*, 291 – 312.
[38] X. Wang, I. M. Chou, W. Hu, R. C. Burruss, *Geochim. Cosmochim. Acta* **2013**, *103*, 1 – 10.
[39] a) P. G. Vekilov, *Cryst. Growth Des.* **2010**, *10*, 5007 – 5019; b) P. G. Vekilov, *Nat. Mater.* **2012**, *11*, 838 – 840.
[40] H. Haberkorn, D. Franke, T. Frechen, W. Goesele, J. Rieger, *J. Colloid Interface Sci.* **2003**, *259*, 112 – 126.
[41] J. Lee, A. Saha, S. Montero-Pancera, A. Kempter, J. Rieger, A. Bose, A. Tripathi, *Langmuir* **2012**, *28*, 4043 – 4046.
[42] A. F. Wallace, L. O. Hedges, A. Fernandez-Martinez, P. Raiteri, J. D. Gale, G. A. Waychunas, S. Whitelam, J. F. Banfield, J. J. De Yoreo, *Science* **2013**, *341*, 885 – 889.
[43] M. P. Schmidt, A. J. Ilott, B. L. Phillips, R. J. Reeder, *Cryst. Growth Des.* **2014**, *14*, 938 – 951.
[44] M. Kellermeier, E. Melero-Garcia, F. Glaab, R. Klein, M. Drechsler, R. Rachel, J. M. Garcia-Ruiz, W. Kunz, *J. Am. Chem. Soc.* **2010**, *132*, 17859 – 17866.
[45] J. D. Rodriguez-Blanco, S. Shaw, L. G. Benning, *Nanoscale* **2011**, *3*, 265 – 271.
[46] N. Koga, Y. Nakagoe, H. Tanaka, *Thermochim. Acta* **1998**, *318*, 239 – 244.
[47] J. Ihli, P. Bots, A. Kulak, L. G. Benning, F. C. Meldrum, *Adv. Funct. Mater.* **2013**, *23*, 1965 – 1973.
[48] a) E. Loste, R. M. Wilson, R. Seshadri, F. C. Meldrum, *J. Cryst. Growth* **2003**, *254*, 206 – 218; b) J. Jiang, M. R. Gao, Y. H. Qiu, S. H. Yu, *Nanoscale* **2010**, *2*, 2358 – 2361.
[49] D. Gebauer, P. N. Gunawidjaja, J. Y. P. Ko, Z. Bacsik, B. Aziz, L. Liu, Y. Hu, L. Bergström, C. W. Tai, T. K. Sham, M. Eden, N. Hedin, *Angew. Chem.* **2010**, *122*, 9073 – 9075; *Angew. Chem. Int. Ed.* **2010**, *49*, 8889 – 8891.
[50] H. S. Lee, T. H. Ha, K. Kim, *Mater. Chem. Phys.* **2005**, *93*, 376 – 382.
[51] a) C. C. Tester, C. H. Wu, S. Weigand, D. Joester, *Faraday Discuss.* **2012**, *159*, 345 – 356; b) C. J. Stephens, S. F. Ladden, F. C. Meldrum, H. K. Christenson, *Adv. Funct. Mater.* **2010**, *20*, 2108 – 2115.
[52] a) B. Guillemet, M. Faatz, F. Gröhn, G. Wegner, Y. Gnanou, *Langmuir* **2006**, *22*, 1875; b) X. R. Xu, A. H. Cai, R. Liu, H. H. Pa, *J. Cryst. Growth* **2008**, *310*, 3779; c) J. Ihli, Y. Y. Kim, E. H. Noel, F. C. Meldrum, *Adv. Funct. Mater.* **2013**, *23*, 1575 – 1585.
[53] A. W. Xu, Q. Yu, W. F. Dong, M. Antonietti, H. Cölfen, *Adv. Mater.* **2005**, *17*, 2217 – 2221.
[54] J. J. J. M. Donners, B. R. Heywood, E. W. Meijer, R. J. M. Nolte, C. Roman, A. P. H. J. Schenning, N. A. J. M. Sommerdijk, *Chem. Commun.* **2000**, 1937 – 1938.
[55] J. Aizenberg, G. Lambert, L. Addadi, S. Weiner, *Adv. Mater.* **1996**, *8*, 222 – 226.
[56] S. E. Wolf, J. Leiterer, V. Pipich, R. Barrea, F. Emmerling, W. Tremel, *J. Am. Chem. Soc.* **2011**, *133*, 12642 – 12649.
[57] a) L. Addadi, S. Raz, S. Weiner, *Adv. Mater.* **2003**, *15*, 959 – 970; b) Y. U. T. Gong, C. E. Killian, I. C. Olson, N. P. Appathurai, A. L. Amasino, M. C. Martin, L. J. Holt, F. H. Wilt, P. U. P. A. Gilbert, *Proc. Natl. Acad. Sci. USA* **2012**, *109*, 6088 – 6093.
[58] See Ref. 10.
[59] J. Ihli, W. C. Wong, E. H. Noel, Y. Y. Kim, A. N. Kulak, H. K. Christenson, M. J. Duer, F. C. Meldrum, *Nat. Commun.* **2014**, *5*, 3169.
[60] J. H. E. Cartwright, A. G. Checa, J. D. Gale, D. Gebauer, C. I. Sainz-Diaz, *Angew. Chem.* **2012**, *124*, 12126 – 12137; *Angew. Chem. Int. Ed.* **2012**, *51*, 11960 – 11970.
[61] A. Fernandez-Martinez, B. Kalkan, S. M. Clark, G. A. Waychunas, *Angew. Chem.* **2013**, *125*, 8512 – 8515; *Angew. Chem. Int. Ed.* **2013**, *52*, 8354 – 8357.
[62] A. L. Goodwin, F. M. Michel, B. L. Phillips, D. A. Keen, M. T. Dove, R. J. Reeder, *Chem. Mater.* **2010**, *22*, 3197 – 3205.
[63] M. Kellermeier, F. Glaab, R. Klein, E. Melero-Garcia, W. Kunz, J. M. Garcia-Ruiz, *Nanoscale* **2013**, *5*, 7054 – 7065.
[64] J. Rieger, *Tenside Surfactants Deterg.* **2002**, *39*, 221 – 225.
[65] Y. W. Wang, Y. Y. Kim, H. K. Christenson, F. C. Meldrum, *Chem. Commun.* **2012**, *48*, 504 – 506.
[66] A. Saha, J. Lee, S. M. Pancera, M. F. Bräu, A. Kempter, A. Tripathi, A. Bose, *Langmuir* **2012**, *28*, 11182 – 11187.
[67] A. E. S. Van Driessche, L. G. Benning, J. D. Rodriguez-Blanco, M. Ossorio, P. Bots, J. M. García-Ruiz, *Science* **2012**, *336*, 69 – 72.
[68] V. V. Hoang, D. Ganguli, *Phys. Rep.* **2012**, *518*, 81 – 140.
[69] J. Rieger, J. Thieme, C. Schmidt, *Langmuir* **2000**, *16*, 8300 – 8305.
[70] J. R. I. Lee, T. Y. J. Han, T. M. Willey, D. Wang, R. W. Meulenberg, J. Nilsson, P. M. Dove, D. J. Terminello, T. van Buuren, J. J. De Yoreo, *J. Am. Chem. Soc.* **2007**, *129*, 10370 – 10381.
[71] a) F. Wang, V. N. Richards, S. P. Shields, W. E. Buhro, *Chem. Mater.* **2014**, *26*, 5 – 21; b) J. Zhang, F. Huang, Z. Lin, *Nanoscale* **2010**, *2*, 18 – 34; c) N. D. Burrows, C. R. H. Hale, R. L. Penn, *Cryst. Growth Des.* **2013**, *13*, 3396 – 3403; d) J. Baumgartner, A. Dey, P. H. H. Bomans, C. Le Coadou, P. Fratzl, N. A. J. M. Sommerdijk, D. Faivre, *Nat. Mater.* **2013**, *12*, 310 – 314; e) L. Zhou, P. O'Brien, *J. Phys. Chem. Lett.* **2012**, *3*, 620 – 628.
[72] a) R. Q. Song, H. Cölfen, *Adv. Mater.* **2010**, *22*, 1301 – 1330; b) L. Zhou, P. O'Brian, *Small* **2008**, *4*, 1566 – 1574.
[73] F. Nudelman, N. A. J. M. Sommerdijk, *Angew. Chem.* **2012**, *124*, 6686 – 6700; *Angew. Chem. Int. Ed.* **2012**, *51*, 6582 – 6596.
[74] F. C. Meldrum, H. Cölfen, *Chem. Rev.* **2008**, *108*, 4332 – 4432.
[75] L. B. Gower, D. J. Odom, *J. Cryst. Growth* **2000**, *210*, 719 – 734.
[76] L. Dai, E. P. Douglas, L. B. Gower, *J. Non-Cryst. Solids* **2008**, *354*, 1845 – 1854.

[77] B. Cantaert, Y. Y. Kim, H. Ludwig, F. Nudelman, N. A. J. M. Sommerdijk, F. C. Meldrum, *Adv. Funct. Mater.* **2012**, *22*, 907 – 915.
[78] J. K. Berg, T. Jordan, H. G. Börner, D. Gebauer, *J. Am. Chem. Soc.* **2013**, *135*, 12512 – 12515.
[79] T. T. Thula, F. Svedlund, D. E. Rodriguez, J. Podschun, L. Pendi, L. B. Gower, *Polymer* **2010**, *3*, 10 – 35.
[80] A. Schenk, H. Zope, Y. Y. Kim, A. Kros, N. A. J. M. Sommerdijk, F. C. Meldrum, *Faraday Discuss.* **2012**, *159*, 327 – 344.
[81] C. Wildebrand, H. Glade, S. Will, M. Essig, J. Rieger, K. H. Büchner, G. Brodt, *Desalination* **2007**, *204*, 448 – 463.
[82] P. Zini, *Polymeric Additives for High Performance Detergents*, Technomic, Lancaster, **1995**.
[83] R. E. Bulo, D. Donadio, A. Laio, F. Molnar, J. Rieger, M. Parrinello, *Macromolecules* **2007**, *40*, 3437 – 3442.
[84] C. G. Sinn, R. Dimova, M. Antonietti, *Macromolecules* **2004**, *37*, 3444 – 3450.
[85] a) F. Fantinel, J. Rieger, F. Molnar, P. Hübler, *Langmuir* **2004**, *20*, 2539 – 2542; b) F. Molnar, J. Rieger, *Langmuir* **2005**, *21*, 786 – 789.
[86] S. Lages, R. Michels, K. Huber, *Macromolecules* **2010**, *43*, 3027 – 3035.
[87] G. A. Tribello, C. Liew, M. Parrinello, *J. Phys. Chem. B* **2009**, *113*, 7081 – 7085.
[88] D. Gebauer, H. Cölfen, A. Verch, M. Antonietti, *Adv. Mater.* **2009**, *21*, 435 – 439.
[89] J. Liu, S. Pancera, V. Boyko, J. Gummel, R. Nayuk, K. Huber, *Langmuir* **2012**, *28*, 3593 – 3605.
[90] M. Kellermeier, H. Cölfen, D. Gebauer, *Methods in Enzymology, Vol. 532* (Ed.: J. J. De Yoreo), Academic Press, Burlington, **2013**, pp. 45 – 69.
[91] a) A. Verch, D. Gebauer, M. Antonietti, H. Cölfen, *Phys. Chem. Chem. Phys.* **2011**, *13*, 16811 – 16820; b) A. Picker, M. Kellermeier, J. Seto, D. Gebauer, H. Cölfen, *Z. Kristallogr.* **2012**, *227*, 744 – 757.
[92] P. Raiteri, R. Demichelis, J. D. Gale, M. Kellermeier, D. Gebauer, D. Quigley, L. B. Wright, T. R. Walsh, *Faraday Discuss.* **2012**, *159*, 61 – 85.
[93] a) S. C. Huang, K. Naka, Y. Chujo, *Langmuir* **2007**, *23*, 12086 – 12095; b) G. B. Cai, G. X. Zhao, X. K. Wang, S. H. Yu, *J. Phys. Chem. C* **2010**, *114*, 12948 – 12954; c) P. B.-Y. Ofir, R. Govrin-Lippman, N. Garti, H. Füredi-Milhofer, *Cryst. Growth Des.* **2004**, *4*, 177 – 183; d) J. Luo, A. Qiu, X. Zhou, R. Lai, P. Dong, X. Xie, *Colloids Surf. A* **2014**, *444*, 81 – 88.
[94] M. J. Olszta, S. Gajjeraman, M. Kaufman, L. B. Gower, *Chem. Mater.* **2004**, *16*, 2355 – 2362.
[95] P. Lipowsky, N. Hedin, J. Bill, R. C. Hoffmann, A. Ahniyaz, F. Aldinger, L. Bergström, *J. Phys. Chem. C* **2008**, *112*, 5373 – 5383.
[96] Y. Jiang, H. Gong, M. Grzywa, D. Volkmer, L. B. Gower, H. Cölfen, *Adv. Funct. Mater.* **2013**, *23*, 1547 – 1555.
[97] C. Sanchez, P. Belleville, M. Popall, L. Nicole, *Chem. Soc. Rev.* **2011**, *40*, 696 – 753.
[98] Y. Oaki, S. Kajiyama, T. Nishimura, H. Imai, T. Kato, *Adv. Mater.* **2008**, *20*, 3633 – 3637.
[99] D. Gebauer, V. Oliynyk, M. Salajkova, J. Sort, Q. Zhou, L. Bergström, G. Salazar-Alvarez, *Nanoscale* **2011**, *3*, 3563 – 3566.
[100] V. Andre, H. Debus, J. Rieger, (BASF AG), Patent WO 2005/094156, **2005**.
[101] A. T. Nagaraja, S. Pradhan, M. J. McShane, *J. Colloid Interface Sci.* **2014**, *418*, 366 – 372.
[102] Z. Jia, Z. Liu, F. He, *J. Colloid Interface Sci.* **2003**, *266*, 322 – 327.
[103] F. Nudelman, E. Sonmezler, P. H. H. Bomans, G. de With, N. A. J. M. Sommerdijk, *Nanoscale* **2010**, *2*, 2436 – 2439.
[104] Y. W. Wang, F. C. Meldrum, *J. Mater. Chem.* **2012**, *22*, 22055 – 22062.
[105] K. Van Vliet, R. Pellenq, M. J. Buehler, J. C. Grossman, H. Jennings, F.-J. Ulm, S. Yip, *MRS Bull.* **2012**, *37*, 395 – 402.
[106] a) C. Vernet, J. Lukasik, E. Prat, *Proceedings of the International Symposium on HPC and RPC* (Eds.: P. C. Aitcin, Y. Delagrave), Sherbrooke, **1998**, pp. 17 – 36; b) V. Morin, F. Cohen-Tenoudji, A. Feylessoufi, P. Richard, *Cem. Concr. Res.* **2002**, *32*, 1907 – 1914.
[107] F. J. Ulm, R. Pellenq, *Damage Mechanics of cementitious materials and structures* (Eds.: G. Pijaudier-Cabot, F. Dufour), Wiley-Blackwell, New York, **2011**, pp. 1 – 18.
[108] M. Vandamme, F. J. Ulm, *Proc. Natl. Acad. Sci. USA* **2009**, *106*, 10552 – 10557.
[109] The cement community uses a notation where letters refer to the oxides: C for CaO, S for SiO_2, H for H_2O, A for Al_2O_3, and F for Fe_2O_3.
[110] B. Lothenbach, G. L. Saout, E. Gallucci, K. Scrivener, *Cem. Concr. Res.* **2008**, *38*, 848 – 860.
[111] I. G. Richardson, *Cem. Concr. Res.* **2004**, *34*, 1733 – 1777.
[112] R. J. M. Pellenq, A. Kushima, R. Shahsavari, K. J. Van Vliet, M. J. Buehler, S. Yip, F. J. Ulm, *Proc. Natl. Acad. Sci. USA* **2009**, *106*, 16102 – 16107.
[113] a) H. F. W. Taylor, *Adv. Cem. Based Mater.* **1993**, *1*, 38 – 46; b) X. Cong, R. J. Kirkpatrick, *Adv. Cem. Based Mater.* **1996**, *3*, 144 – 156; c) I. G. Richardson, G. W. Groves, *Cem. Concr. Res.* **1993**, *23*, 999 – 1000; d) H. F. W. Taylor, *Z. Kristallogr.* **1992**, *202*, 41 – 50; e) A. Nonat, *Cem. Concr. Res.* **2004**, *34*, 1521 – 1528; f) J. J. Thomas, H. M. Jennings, A. J. Allen, *J. Phys. Chem. C* **2010**, *114*, 7594 – 7601.
[114] a) L. Pegado, C. Labbez, S. V. Churakov, *J. Mater. Chem. A* **2014**, *2*, 3477 – 3483; b) I. García-Lodeiro, A. Fernández-Jiménez, A. Palomo, *Eco-Efficient Concrete* (Eds.: F. Pacheco-Torgal, S. Jalali, J. Labrincha, V. M. John), Woodhead, Cambridge, **2013**, pp. 439 – 487; c) I. Garcia-Lodeiro, A. Fernadez-Jimenez, A. Palomo, *Cem. Concr. Res.* **2013**, *52*, 112 – 122.
[115] *Cement-Based Materials for Nuclear Waste Storage* (Eds.: C. Cau-dit-Coumes, F. Frizon, S. Lorente), Springer, New York, **2013**.
[116] H. M. Jennings, *Cem. Concr. Res.* **2008**, *38*, 275 – 289.
[117] L. Nicoleau, *Cem. Concr. Res.* **2011**, *41*, 1339 – 1348.
[118] C. Plassard, E. Lesniewska, I. Pochard, A. Nonat, *Langmuir* **2005**, *21*, 7263 – 7270.
[119] C. Labbez, B. Jönsson, I. Pochard, A. Nonat, B. Cabane, *J. Phys. Chem. B* **2006**, *110*, 9219 – 9230.
[120] B. Jönsson, H. Wennerström, A. Nonat, B. Cabane, *Langmuir* **2004**, *20*, 6702 – 6709.
[121] B. Jönsson, A. Nonat, C. Labbez, B. Cabane, H. Wennerström, *Langmuir* **2005**, *21*, 9211 – 9221.
[122] a) A. C. A. Muller, K. L. Scrivener, A. M. Gajewicz, P. J. McDonald, *J. Phys. Chem. C* **2013**, *117*, 403 – 412; b) J. J. Thomas, H. M. Jennings, A. Allen, *Cem. Concr. Res.* **1998**, *28*, 897 – 905; c) P. J. McDonald, J. Mitchell, M. Mulheron, P. S. Aptaker, J. P. Korb, L. Monteillet, *Cem. Concr. Res.* **2007**, *37*, 303 – 309.
[123] Y. Ohama, *Cem. Concr. Compos.* **1998**, *20*, 189 – 212.
[124] R. Morlat, G. Orange, Y. Bomal, P. Godard, *J. Mater. Sci.* **2007**, *42*, 4858 – 4869.
[125] Y. Ohama in *Handbook of Polymer-Modified Concrete and Mortars* (Ed.: V. Ramachandran), Noyes, Park Ridge, **1995**.
[126] A. Franceschini, S. Abramson, V. Mancini, B. Bresson, C. Chassenieux, N. Lequeux, *J. Mater. Chem.* **2007**, *17*, 913 – 922.
[127] a) J. Minet, S. Abramson, B. Bresson, C. Sanchez, V. Montouillout, N. Lequeux, *Chem. Mater.* **2004**, *16*, 3955 – 3962; b) J. Minet, S. Abramson, B. Bresson, A. Franceschini, H. Van Damme, N. Lequeux, *J. Mater. Chem.* **2006**, *16*, 1379 – 1383.
[128] J. J. Beaudoin, L. Raki, R. Alizadeh, *Cem. Concr. Compos.* **2009**, *31*, 585 – 590.

[129] B. Theng, *Formation and Properties of Clay Polymer Composites*, Elsevier, New York, **1979**.
[130] F. Merlin, H. Lombois, S. Joly, N. Lequeux, J. L. Halary, H. Van Damme, *J. Mater. Chem.* **2002**, *12*, 3308 – 3315.
[131] H. Matsuyama, J. F. Young, *Chem. Mater.* **1999**, *11*, 16 – 19.
[132] a) C. Giraudeau, J. B. D'Espinose De Lacaillerie, Z. Souguir, A. Nonat, R. J. Flatt, *J. Am. Ceram. Soc.* **2009**, *92*, 2471 – 2488; b) J. Plank, H. Keller, P. R. Andres, Z. Dai, *Inorg. Chim. Acta* **2006**, *359*, 4901 – 4908.
[133] a) J. J. Thomas, H. M. Jennings, J. J. Chen, *J. Phys. Chem. C* **2009**, *113*, 4327 – 4334; b) S. Bishnoi, K. L. Scrivener, *Cem. Concr. Res.* **2009**, *39*, 849 – 860.
[134] S. Garrault-Gauffinet, A. Nonat, *J. Cryst. Growth* **1999**, *200*, 565 – 574.
[135] A. Picker, Ph.D. thesis, University of Konstanz (Germany), **2012**.
[136] a) P. Nieto, H. Zanni, *J. Mater. Sci.* **1997**, *32*, 3419 – 3425; b) F. Gaboriaud, A. Nonat, D. Chaumont, A. Craievich, B. Hanquet, *J. Phys. Chem. B* **1999**, *103*, 2091 – 2099.
[137] P. Noel, R. Rixom, *Chemical Admixtures for Concrete*, *3rd ed.*, E&FN Spon, London, **1999**.
[138] M. Zajac, A. Nonat, J. P. Korb, *Proceedings of the 12th ICCC*, Montreal, **2007**.
[139] S. Garrault, A. Nonat, *Langmuir* **2001**, *17*, 8131 – 8138.
[140] L. Nicoleau, A. Nonat, *Cem. Concr. Res.* **2012**, *42*, 881 – 887.
[141] Ordinary Portland cement is largely or almost fully hydrated at this time.
[142] M. Duriez, *Ann. Inst. Tech. Batim. Trav. Publics* **1956**, *98*, 482 – 483.
[143] a) O. Bayard, U. Holland, D. Dressel, H. M. Ludwig, *Proceedings of the 18th IBAUSIL*, Weimar, **2012**, pp. 338 – 345; b) M. H. Hubler, J. J. Thomas, H. M. Jennings, *Cem. Concr. Res.* **2011**, *41*, 842 – 846.
[144] L. Nicoleau, T. Gaedt, L. Chitu, G. Maier, O. Paris, *Soft Matter* **2013**, *9*, 4864 – 4874.
[145] Master X-Seed marketed by BASF can be found under http://www.basf-cc.ae/en/Literatures/Brochures/Pages/MasterX-Seed-Solutions.aspx.
[146] P. Domínguez-García, M. A. Rubio, *Colloids Surf. A* **2010**, *358*, 21 – 27.
[147] H. P. Koch, *Pharmazie* **1993**, *48*, 643 – 659 (and references therein).
[148] B. Jefferson, P. R. Jarvis, *Interface Science in Drinking Water Treatment* (Eds.: G. Newcombe, D. Dixon), Elsevier, Amsterdam, **2006**, pp. 45 – 61.
[149] D. Napper, *J. Colloid Interface Sci.* **1977**, *58*, 390 – 407.
[150] a) M. Sarikaya, C. Tamerler, A. Y. Jen, K. Schulten, F. Baneyx, *Nat. Mater.* **2003**, *2*, 577 – 585; b) C. Tamerler, D. Khatayevich, M. Gungormus, T. Kacar, E. E. Oren, M. Hnilova, M. Sarikaya, *Biopolymers* **2010**, *94*, 78 – 94.
[151] A. Picker, L. Nicoleau, A. Nonat, C. Labbez, H. Cölfen, *Adv. Mater.* **2014**, *26*, 1135 – 1140.
[152] J. M. Lehn, *C. R. Chim.* **2011**, *14*, 348 – 361, and references therein.
[153] P. Sajanlal, T. Pradeep, *Nano Res.* **2009**, *2*, 306 – 320.
[154] S. Deng, V. Tjoa, H. M. Fan, H. R. Tan, D. C. Sayle, M. Olivo, S. Mhaisalkar, J. Wei, C. H. Sow, *J. Am. Chem. Soc.* **2012**, *134*, 4905 – 4917.
[155] X. Wu, S. Xiong, Z. Liu, J. Chen, J. C. Shen, T. Li, P. Wu, P. Chu, *Nat. Nanotechnol.* **2011**, *6*, 103 – 106.
[156] T. Tachikawa, P. Zhang, Z. Bian, T. Majima, *J. Mater. Chem. A* **2014**, *2*, 3381 – 3388.
[157] Z. Bian, T. Tachikawa, P. Zhang, M. Fujitsuka, T. Majima, *Nat. Commun.* **2014**, *5*, 1 – 9.
[158] a) H. D. Espinosa, J. E. Rim, F. Barthelat, M. J. Buehler, *Prog. Mater. Sci.* **2009**, *54*, 1059 – 1100; b) E. Munch, M. E. Launey, D. H. Alsem, E. Saiz, A. P. Tomsia, R. O. Ritchie, *Science* **2008**, *322*, 1516 – 1520.
[159] F. Natalio, T. P. Corrales, M. Panthöfer, D. Schollmeyer, I. Lieberwirth, W. E. G. Müller, M. Kappl, H. J. Butt, W. Tremel, *Science* **2013**, *339*, 1298 – 1302.
[160] D. Gebauer, *Angew. Chem.* **2013**, *125*, 8366 – 8367; *Angew. Chem. Int. Ed.* **2013**, *52*, 8208 – 8209.
[161] A. Picker, L. Nicoleau, A. Nonat, C. Labbez, H. Cölfen, *Proceedings of the 11th International Materials Research Congress*, Cancun, **2012**.
[162] K. L. Scrivener, A. Nonat, *Cem. Concr. Res.* **2011**, *41*, 651 – 665.
[163] H. M. Jennings, J. W. Bullard, *Cem. Concr. Res.* **2011**, *41*, 727 – 735.
[164] J. S. Dolado, K. van Breugel, *Cem. Concr. Res.* **2011**, *41*, 711 – 726.
[165] a) M. Kellermeier, H. Cölfen, J. M. Garcia-Ruiz, *Eur. J. Inorg. Chem.* **2012**, 5123 – 5144; b) W. Noorduin, A. Grinthal, L. Mahadevan, J. Aizenberg, *Science* **2013**, *340*, 832 – 837.